NASA CONTRACTOR
REPORT

NASA CR-162049

TRANSIENT AND DIFFUSION ANALYSIS OF HgCdTe

By J. C. Clayton
Semtec, Incorporated
555 Sparkman Drive
Huntsville, Alabama

Annual Report

July 1982

Prepared for:

NASA-Marshall Space Flight Center
Marshall Space Flight Center, Alabama 35812

TECHNICAL REPORT STANDARD TITLE PAGE

1. REPORT NO.	2. GOVERNMENT ACCESSION NO.	3. RECIPIENT'S CATALOG NO.
NASA CR-162049		

4. TITLE AND SUBTITLE	5. REPORT DATE
Transient and Diffusion Analysis of HgCdTe	July 1982
	6. PERFORMING ORGANIZATION CODE
7. AUTHOR(S)	8. PERFORMING ORGANIZATION REPORT #
J. C. Clayton	
9. PERFORMING ORGANIZATION NAME AND ADDRESS	10. WORK UNIT NO.
Semtec, Inc. 555Sparkman Drive Huntsville, Alabama	11. CONTRACT OR GRANT NO. NAS8-33698
	13. TYPE OF REPORT & PERIOD COVERED
12. SPONSORING AGENCY NAME AND ADDRESS	Contractor Report Annual
National Aeronautics and Space Administration Washington, DC 20546	14. SPONSORING AGENCY CODE

15. SUPPLEMENTARY NOTES

16. ABSTRACT

This work addresses the problem of solute redistribution during directional solidification of HgCdTe. Both one-dimensional and two-dimensional models for solute redistribution are treated and model results compared to experiment. The central problem addressed is the cause of radial inhomogeneities found in directionally solidified HgCdTe. A large scale gravity-driven interface instability, termed "shape instability," is postulated to be the cause of radial inhomogeneities. Recommendations for future work, along with appropriate computer programs,are included in this report.

17. KEY WORDS	18. DISTRIBUTION STATEMENT
	Unclassified-Unlimited S C McKannan for Lowell K. Zoller, Dir, LA01

19. SECURITY CLASSIF. (of this report)	20. SECURITY CLASSIF. (of this page)	21. NO. OF PAGES	22. PRICE
Unclassified	Unclassified	140	NTIS

MSFC - Form 3292 (May 1969)

For sale by National Technical Information Service, Springfield, Virginia 22151

TABLE OF CONTENTS

1.0 INTRODUCTION

This report is a summary of the past year's effort under Contract NAS8-33698, entitled "Transient and Diffusion Analysis of HgCdTe". The primary purpose of this work is to provide analysis and computational support for a proposed Materials Processing in Space flight project involving crystal growth of mercury cadmium telluride alloys under microgravity conditions. The overall goal of this flight project is to obtain homogeneous material with minimum radial and axial compositional variations. Accordingly, this work addresses the problem of solute redistribution during directional solidification of HgCdTe.

This work reports on new results obtained using the one-dimensional model, the interface deconvolution model, and addresses the problem of two dimensional diffusion and shape instability.

Two papers have been submitted for publication and preliminary copies of these will be included in the appendix. In addition, computer code for the models discussed here is documented and issued under a separate cover to the appropriate NASA personnel. This report contains experimental data from the work of Dr. D.C. Gillies, formerly with USRA/MSFC, and is included for comparison with the model predictions.

2.0 BACKGROUND

The solid solution semiconductor HgCdTe has emerged as the premier variable energy gap intrinsic infrared detector material for the future. Considering $Hg_{1-x}Cd_xTe$ as a mixed crystal of HgTe and CdTe, the material properties, including the bandgap, may be varied by changing the solute (CdTe) mole fraction x. The bandgap varies linearly with x from approximately -.3eV (x=0, semimetal) to 1.6eV (x=1, CdTe) allowing selection of a suitable proportions of HgTe and CdTe.

It is this property, however, that is the source of one of the primary problems in the growth of high quality HgCdTe. Requirements for large area focal plane arrays for IR detectors necessitate compositional uniformities of $\Delta x < .01$ or less over a crystal slice of diameter 1cm. or larger. Compositional variations, either radial or longitudinal, lead to variations in bandgap and thus detector response over the area of the detector. Growth techniques that eliminate or minimize compositional variations are of primary importance in producing state-of-the-art material capable of meeting detector performance requirements.

In order to produce more homogeneous material we must first understand and quantify the causes of compositional variations in HgCdTe. Although several growth techniques have been investigated by other workers, we concentrate on growth by directional solidification as this offers a high potential yield of material from a relatively simple growth technique. Directional solidifi-

cation of HgCdTe results in a solute (CdTe) profile that is characterized by a mean axial solute distribution with an initial transient region, a steady-state or near steady-state region depending on ampoule pull rate, and a final transient region characterized by a decreasing CdTe concentration as the end of the ampoule is reached. This indicates that the primary means of solute redistribution in HgCdTe is via diffusion through a diffusion layer ahead of the solid-liquid interface.

Concentrating on the axial solute profile, SEMTEC has developed a one-dimensional model based on the diffusion equation to predict the axial solute distribution in a finite length ampoule. The model assumes a planar interface and linear thermal field, but accounts for variations in the segregation coefficient and interface temperature with composition, factors that are particularly important in HgCdTe. The model also calculates a growth velocity determined by the thermal field and interface concentration rather than assuming a constant growth velocity equal to the pull rate.

The inputs to the one dimensional model are the phase diagram (pseudo-binary), ampoule pull rate and length, initial solute concentration, and the effective diffusion constant

(taken independently of temperature and concentration). The model gives axial solute concentration in the solid, interface position, and interface velocity at each chosen time interval. By comparing experimental solute profiles to the model results for various values of the diffusion constant, we have arrived at a value of D between $5 \times 10^{-5} cm^2/sec$ and $7 \times 10^{-5} cm^2/sec$ for a wide range of ampoule pull rates (.076 cm/hr to .41 cm/hr). The degree of agreement between experiment and theory is quite good, confirming that the axial solute distribution is dominated by diffusion for HgCdTe.

Details of the model are given in a paper submitted for publication and included in the appendix of this report. Results obtained this year using the model will be addressed in a later section of this report.

Further examination of the solute distribution in Bridgman growth HgCdTe reveals that there is a significant radial variation in the solute. This radial variation is present in crystals grown under a variety of thermal conditions and growth rates. Although axial solute variations are an unavoidable consequence of diffusion limited growth, it should be possible to eliminate radial variations under the proper growth conditions, at least during steady state growth. The causes of this radial solute variation is a key issue in the ground based HgCdTe research effort.

Experimental results to date indicate that in the steady

state growth region, the isoconcentration lines are concave (concentration of CdTe at r=o is less than at the crystal outer surface). The isoconcentration lines are not perfectly axisymmetric, indicating misalignment of the ampoule axis with the g-vector and/or thermal field.

It is appropriate at this point to indicate some fundamental observations regarding solute redistribution. In the steady state growth region we have (by difinition) no variation in the axial solid composition at a fixed radius, i.e. the solid concentration is a function of the radial variable r alone. If the interface is an isotherm, then it is also an isoconcentrate and homogeneous material results. Conversely, if the interface is found to be an isoconcentrate, then it must be an isotherm and homogeneous material results. As a corollary, if radial composition variations are present in the steady-state region, the interface must be neither an isotherm nor an isoconcentrate, a situation which complicates the analysis of the growth behavior.

Since radial compositional variations are observed in HgCdTe samples, we must seek the cause of these variations in order to ascertain whether appropriate growth techniques may eliminate them. Several factors may influence the steady-state solute distribution; the thermal field, interface shape, convection, and diffusion may all play a part in determining steady

state conditions. An additional mechanism for solute redistribution in the HgCdTe system has been postulated. Consider a system such as HgCdTe in which the rejected component (HgTe) is more dense than the bulk fluid. As a diffusion layer is built up during growth, a layer of HgTe rich liquid is established just ahead of the solid-liquid interface. If the interface becomes curved, say concave, the heavier HgTe rich liquid will flow along the interface and concentrate at the lowest point along the interface, leaving the center of the interface HgTe rich as compared to the outer edges. As HgTe is also the lower melting point element in the pseudobinary system HgTe-CdTe, the solidus temperature of the center of the interface is lowered with respect to the interface edges (for a concave interface). As the temperature increases as we move away from the interface into the liquid, this solute profile will result in an increase in curvature (more concave) in the interface. This is a dynamic process that once begun leads to interface of increasing curvature limited only by thermal consideration. Similar arguments apply if we consider a convex interface with accumulation of HgTe at the edges of the sample. This "shape instability" was first postulated for the HgCdTe system by Davidson (1) as a possible cause of radial compositional variations.

We will briefly address each of the above mentioned mechanisms for radial solute redistribution in the following pages and provide model results and experimental details in later

sections of this report.

The thermal field is important initially as it determines the location and shape of the initial interface. Assuming nucleation and faceting effects do not effect the growth process after some time interval, then the first to freeze portion freezes out of a liquid of composition near C_o (taken to be x= .20 in most experiments) at a temperature of nearly 800°C. Furnace temperatures are generally chosen to yield the steady state solidification isotherms (705°C for C_o=.20) at the middle of the adiabatic zone, and thus one might initially suspect that the first to freeze portion occurs above the adiabatic zone with a convex isotherm. However, initially the thermal coupling between the ampoule and the cold zone in the furnace is poor since only a small portion, if any, of the ampoule is in the cold zone. This shifts the isotherms downward in the furnace and may result in initial freezing well down in the cold zone. Thermal problems of this nature are difficult to model since the heat transfer characteristics are highly dependent on how the ampoule is constructed and supported in the furnace; experiments using model materials in an instrumented ampoule are needed to determine the early thermal behavior.

Independent of the location in the furnace that the first to freeze occurs, it is evident that it is difficult to set experimental conditions such that the solid-liquid interface

remains on a planar isotherm. Given that the interface likely becomes curved on approach to steady-state, shape instability and/or lateral diffusion along a curved interface will result in radial compositional variations in the steady state region. Due to the high vapor pressures encountered in HgCdTe, it is difficult to instrument the ampoule with thermocouple or electrodes for Peltier pulsing. We must use other techniques to determine the interface shape and concentration.

We find ourselves in the position of realizing that the steady-state solute distribution depends greatly on the initial stages of growth, and yet cannot adequately predict the initial behavior due to complicated thermal fields and nucleation behavior. Thermal modeling of the steady-state region in which isothermal boundary conditons can be applied to the ampoule some distance away from the interface is on a firmer footing. We also recognize that chemical analysis indicates that there are radial composition variations in the steady-state, thus the interface is neither given by the shape of the isotherms nor the isoconcentrates. Since we may predict with some confidence the thermal field at steady state and experimentally measure the concentration field in the grown crystal, we may use this information to "deconvolute" the existing interface shape at any point in the steady state region.

Details of the deconvolution technique are given in a paper submitted for publication which is included as an appendix to this report. Examples of the results obtained from the deconvolution process are given in a later section of this report. The basic principle of interface deconvolution is based on the observation that the solid-liquid interface is the locus of all points in the sample whose solidification temperature coincides with the thermal field in the sample at a particular time. Let $C_s(x,y)$ be the solid composition profile measured on the crystal. The solidus curve of the phase diagram may be used to obtain $(S(C_s(x,y))$ where S is the solidus temperature corresponding to the concentration $C_s(x,y)$ and we assume no undercooling. By appropriate use of a thermal model we may calculate the thermal field present in the crystal $T(x,y)$. We thus have two temperature distributions in the crystal at any point in time, the temperature at which each point froze $S(C_s(x,y))$ and the calculated temperature at each point in the crystal $T(x,y)$. The interface is determined as those points at which $S(C_s(x,y))$ is equal to $T(x,y)$.

In actual practice we must use an iterative procedure to accurately determine the interface location since the interface represents a change in thermal conductivity and is thus a

boundary condition to be applied in the thermal model. Details of this iterative procedure are given in the appendix. The result of the deconvolution process is an interface location and solute concentration along the interface that is self-consistent with the thermal boundary conditions and measured solute concentration profiles.

Once a steady-state interface shape and composition have been established, we may seek to discover the causes of the compositional variations along the interface. It is known that lateral diffusion along a curved interface may lead to radial variations in solute redistribution. Coriell, Sekerka, et al (2) have addressed the problem of solute redistribution by diffusion along a curved interface. They assumed an interface shape and calculated the resulting interface solute profile due to lateral diffusion. Note that it is not necessary to determine the thermal field to solve this problem; the assumed interface shape and resulting composition may not be consistent with thermal boundary conditions encountered in an experiment. The work of Coriell and Sekerka has been applied to HgCdTe and sample calculations are given in a later section of this report. Based on preliminary experimental work and applying Coriell and Sekerka's calculations, it does not appear that lateral diffusion alone can account for the magnitude of radial segregation found in HgCdTe samples. We must then address the

mechanism of shape instability to ascertain if gravity driven flow along the interface is the cause of these compositional variations. In a later section, the appropriate equations are developed and certain conservation conditions are derived pertaining to shape instability.

The work thus far has followed a logical sequence. The one dimensional model is applied to determine an effective diffusion constant and to investigate the influence of various processing parameters such as pull rate and gradient on the axial profile. Two dimensional interface deconvolution is used to estimate the magnitude of interface curvature that leads to radial inhomogeneities. Once an approximate interface shape is established, we can apply two dimensional diffusion calculations to determine if diffusion is the dominant mechanism for radial solute variations. Finally we address the problem of shape instability and develop appropriate equations suitable for numerical solution. In the following sections we present calculational and experimental details concerning each of these topics.

3.0 ONE DIMENSIONAL TRANSIENT ANALYSIS

Details of the one dimensional transient analysis program are given in the appendix to this report. Previous results are also given in a report for contract NAS8-33698 dated 20 December 1980.

3.1 RESULTS USING ONE DIMENSIONAL TRANSIENT ANALYSIS

The first objective of the 1-D program was to determine the effective diffusion coefficient. For this the original intention was to utilize both initial and final transient regions of crystals grown at constant translation rate. For reasons to be explained this procedure did not lead to good results with the initial transient and other procedures involving changes in the translation rate and stopping the crystal during growth were devised. Some of the most recent uses of the program will be described in the following sections. The implication of the results on the design of future growth experiments will be stressed.

3.2. UNINTERRUPTED DIRECTIONAL SOLIDIFICATION

Many sets of data have been calculated using as variables the translation rate, the length of the ampoule, the effective diffusion coefficient and the nominal composition.

Results typical of what the model can achieve are shown in Figures 1-4. To illustrate the program a 20cm crystal of $Hg_{0.80}Cd_{0.20}Te$ was "solidified" in a gradient of 200°C/cm at a constant translation rate of 2mm/hour. Figure 1 shows the

Figure 1

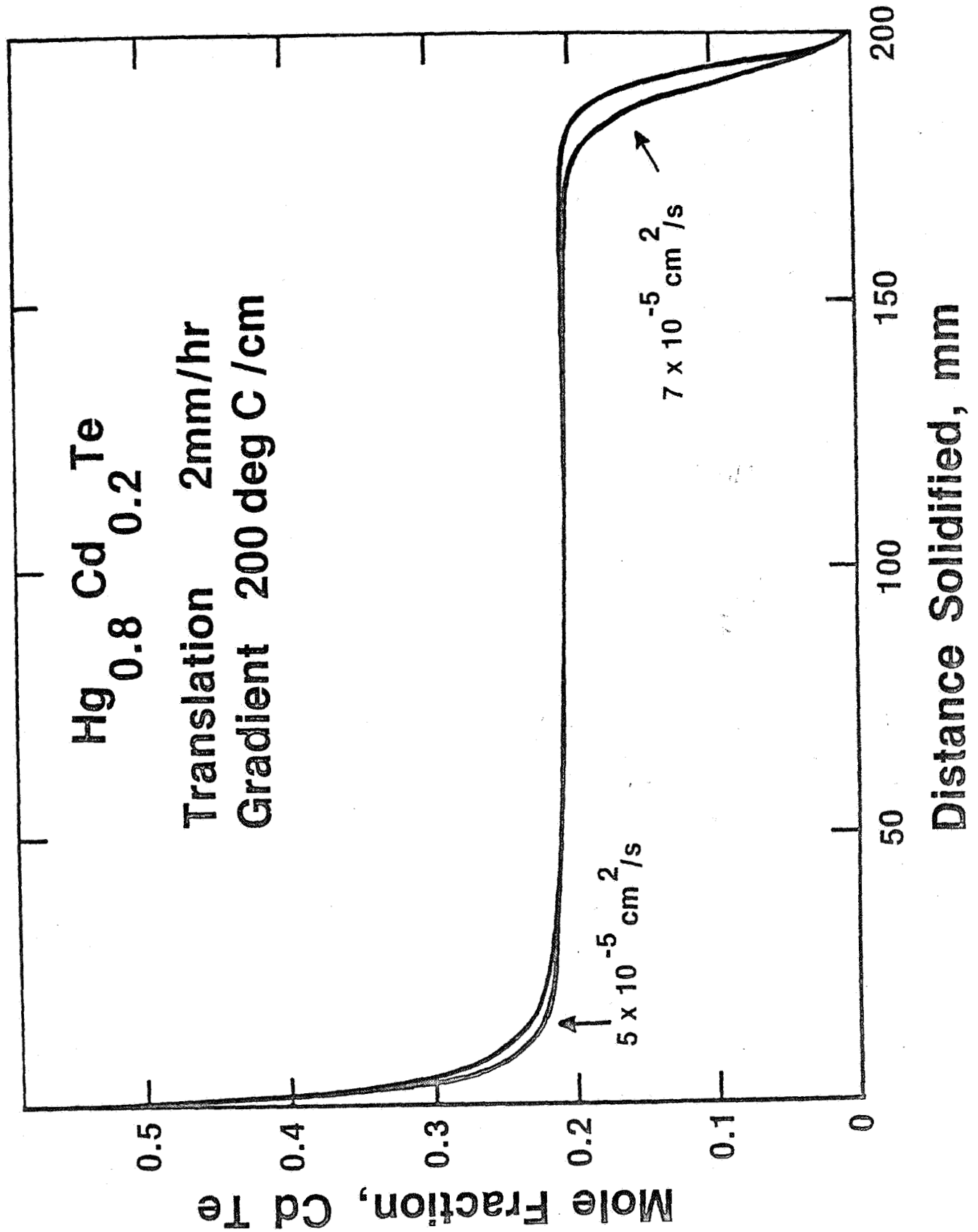
Hg0.8 Cd0.2 Te
Translation 2mm/hr
Gradient 200 deg C /cm
5 x 10-5 cm2/s
7 x 10-5 cm2/s
Mole Fraction, Cd Te
0.5
0.4
0.3
0.2
0.1
0
50
100
150
200
Distance Solidified, mm

composition along the length of the crystal assuming diffusion coefficients of $5 \times 10^{-5} cm^2/sec$ and $7 \times 10^{-5} cm^2/sec$. A clear distinction can be seen particularly in the region of the final transient. The value during the so-called steady state region never quite reaches the nominal value of 0.20; this is due to series truncation which builds up during the numerical analysis. Absolute accuracy must be traded off against excessive program running time to reach a representative result.

Other data from this model are shown in Figure 2. The location of the interface demonstrates solidification initiating high up in the hot zone of the furnace and proceeding down to the mid-plane (0 on the graph) where steady state solidification takes place. In the final transient the interface moves down into the cold end where the mercury rich material freezes.

Figure 2 also illustrates the interface velocity which reaches a maximum equal to the translation rate only during steady state solidification and during the very last moment of crystal growth when the melt is completely depleted of cadmium. The decrease and subsequent increase in the velocity during the final transient occurs as a result of the inflexion point in the composition data as shown in Figure 1. As the final transient regime is entered the interface moves down into the cold zone to solidify liquid which can no longer be replenished by diffusion with cadmium. The interface thus moves slower than the pull rate. However towards the end of growth the liquid composition tends asymptotically

Figure 2

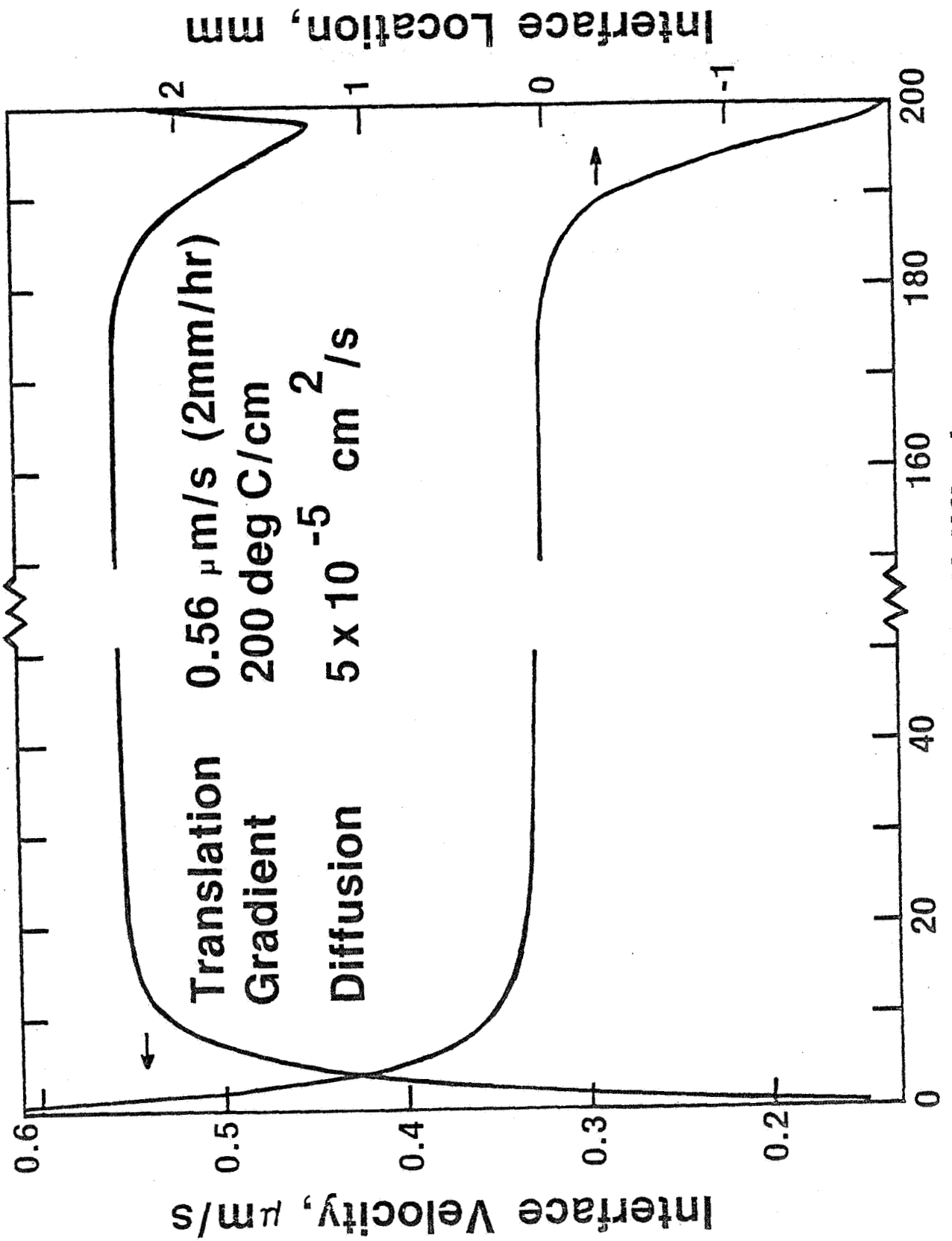
Interface Location, mm
2
1
0
-1
Translation 0.56 μm/s (2mm/hr)
Gradient 200 deg C/cm
Diffusion 5 x 10^-5 cm^2/s
Interface Velocity, μm/s
0.6
0.5
0.4
0.3
0.2
0
20
40
160
180
200
Distance Solidified, mm

to the mercury telluride composition which will grow at the translation rate. The interface velocity thus increases.

The effect of varying the temperature gradient was also calculated. Several different, but plausible, temperature gradients were input as data and the resulting transient analysis curves for 100°C/cm and 400°C/cm are shown in Figure 3 for a sample pull rate of 2mm/hr. and a diffusion constant of 7×10^{-5} cm^2/sec. In comparison to varying the diffusion coefficient, which has a large effect on the results, it can be seen that the shapes of the transient analysis curves are not altered much by gradient. This result has important implications, in that the gradient within a silica ampoule loaded with HgCdTe cannot be measured with any degree of accuracy. Thus, a reasonable value for the effective diffusion coefficient can be obtained due to the high sensitivity of D and the low sensitivity of G, the temperature gradient.

There is one other variable which enters into the transient analysis equations, namely translation rate. Figure 4 shows the effect of varying the translation rate over several orders of magnitude. These curves are important in that they give immediate information as to what the minimum translation rate must be to expect any steady state growth in the crystal. There are also implications here as to the desirable length of ampoule and the trade off between translation rate and ampoule length. A trade

Figure 3

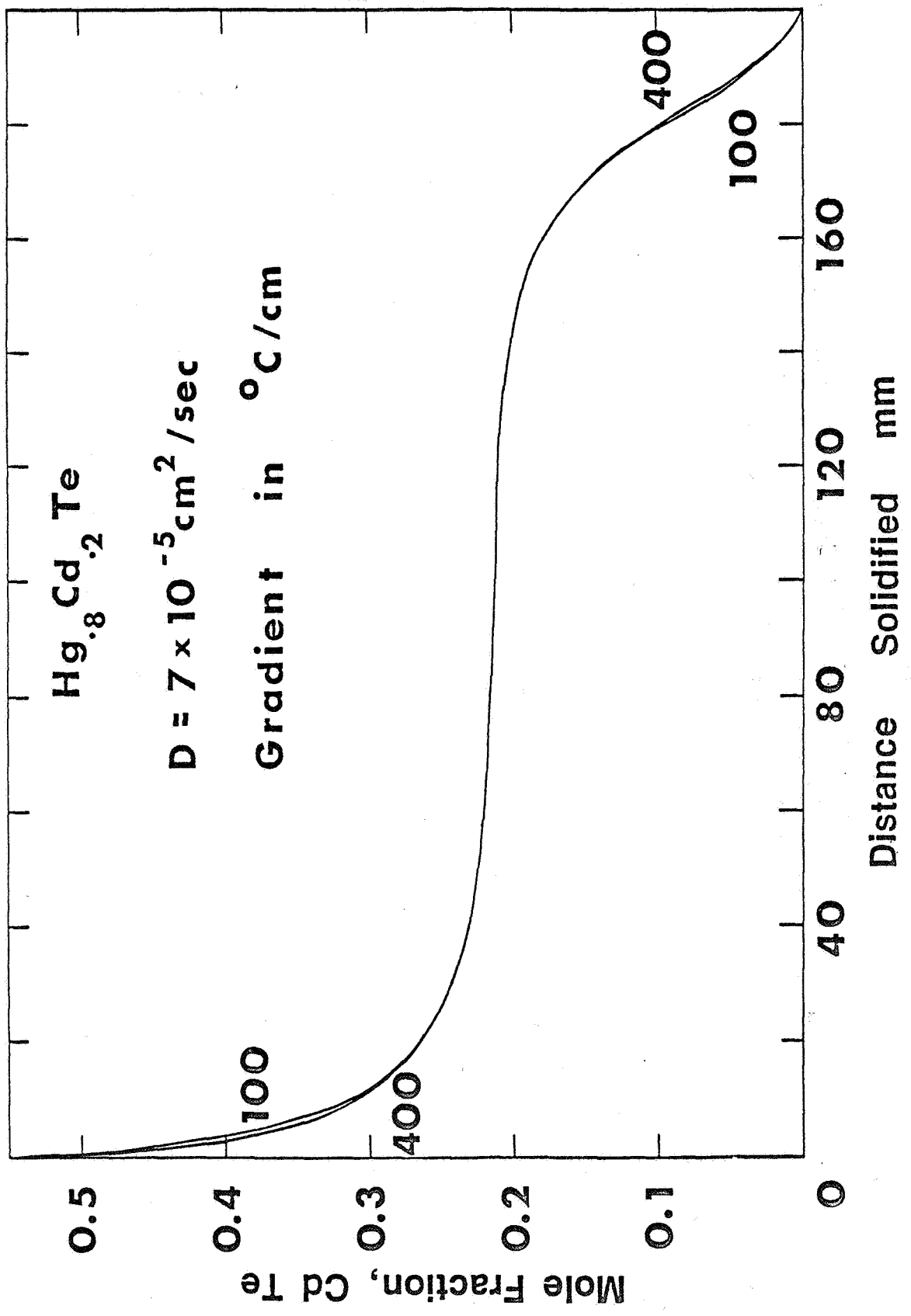
Hg.8Cd.2 Te
D = 7 x 10-5cm2/sec
Gradient in °C/cm
100
400
400
100
Mole Fraction, Cd Te
0.5
0.4
0.3
0.2
0.1
0
40
80
120
160
Distance Solidified mm

Figure 4

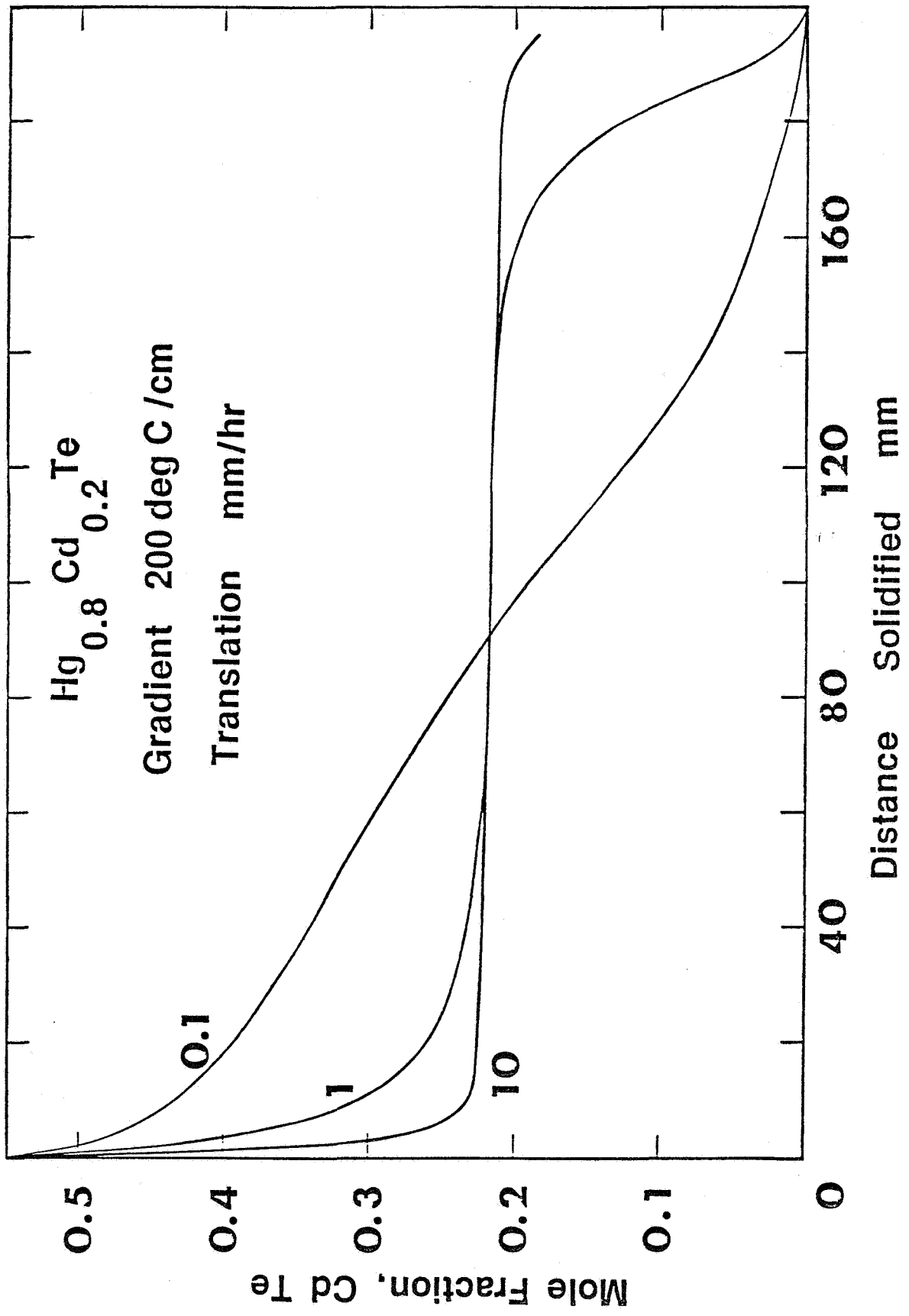
Hg0.8 Cd0.2 Te
Gradient 200 deg C /cm
Translation mm/hr
0.1
1
10
Mole Fraction, Cd Te
0.5
0.4
0.3
0.2
0.1
0
40
80
120
160
Distance Solidified mm

off exists between translation rate, thermal gradient, and ampoule length. As the translation rate is increased, the thermal gradient necessary to avoid constitutional supercooling increases. On the other hand, decreasing the pull rate results in longer transient regions with a corresponding shorter steady state region for a fixed ampoule length. The one dimensional model is well suited for choosing proper growth parameters prior to actual growth experiments.

Data pertaining to a real crystal together with the compositional data of the same crystal are shown in Figure 5. This crystal was grown at NASA by Dr. L.R. Holland of Athens State College. Translation rate of 0.762mm/hr is slower than the 2mm/hr used in the example of Figure 1 and the transient regions are somewhat longer. For the diffusion coefficient of $7 \times 10^{-5} cm^2/sec$ it is evident that there is little steady state region. The crystal exhibits end effects before the initial transient is completed. Assuming this diffusion coefficient, a much longer crystal than this would have to be grown to ensure a reasonable length grown in the steady state regime. Compositional data for the real crystal demonstrate a reasonable fit except in the initial transient region. There are several reasons for the initial fit being bad. The two main ones are as follows.

1. The ampoule was designed with a conical end in order to encourage the growth of a single crystal from the first to freeze nucleus. The model, however, assumes a flat interface and in the

Figure 5

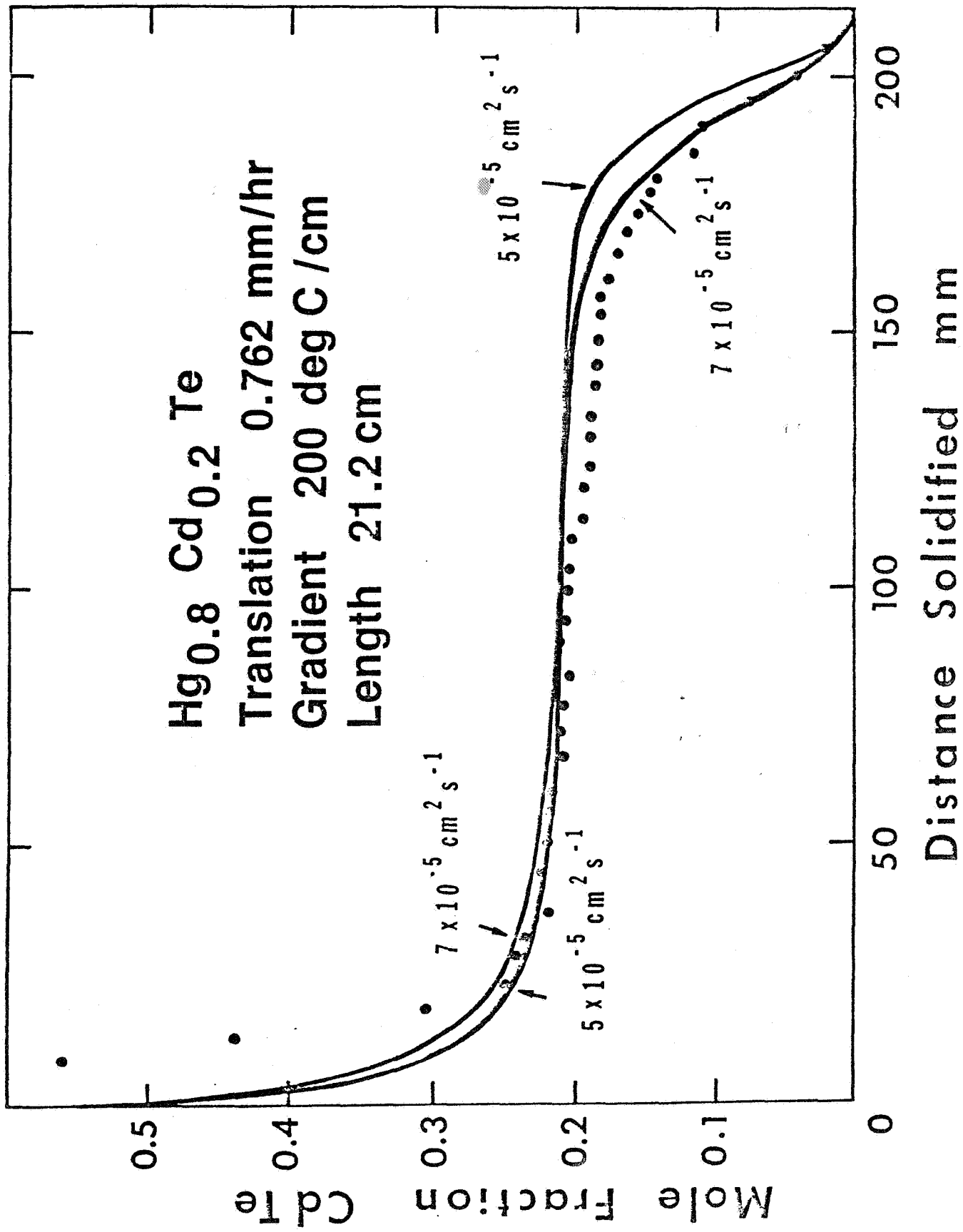
Hg0.8 Cd0.2 Te
Translation 0.762 mm/hr
Gradient 200 deg C /cm
Length 21.2 cm
7 x 10-5 cm2 s-1
5 x 10-5 cm2 s-1
5 x 10-5 cm2 s-1
7 x 10-5 cm2 s-1
Mole Fraction Cd Te
0.5
0.4
0.3
0.2
0.1
0
50
100
150
200
Distance Solidified mm

initial transient region during which the interface moves towards the cold end there is little chance of this occurring especially with a changing cross-section.

2. It was evident from other results that nucleation did not take place at the tip of the ampoule. The starting point for unidirectional solidification is thus ill defined, making comparison to model results difficult.

Once nucleation has taken place and solidification occurs in the cylindrical section of the ampoule the experimental data fall much closer to the model. The experimental results shown here represent a mean of nine points taken with a scanning electron microscope fitted with energy dispersive spectrometry. As these readings are taken on a cross-section a flat interface is assumed. However, radial solute variations do exist and thus these data represent the mean axial solute distribution. The final transient shows a good fit to the diffusion coefficient of $7 \times 10^{-5} cm^2/sec$. Further details of this fitting may be found in the paper included in the appendix.

The use of the model in the direct mode results in determining effective diffusion coefficients, optimum translation rates and crystal lengths for obtaining a reasonable length of crystal grown in the steady state. An assumption is made here as to a known thermal gradient and, more important, a flat interface. For a given gradient it is possible to approximate the fastest translation rate before breakdown takes place. By applying the classical con-

stitutional supercooling criteria, we find a temperature gradient of 170°C/cm is needed to grow crystals at 5mm/hour assuming $D=7\times10^{-5}cm^2/sec$. It was found, however, that a crystal grown at 4mm/hour exhibited dendritic growth. There may have been several reasons for this. A gradient of 180°C/cm was measured in an empty silica ampoule. In reality the gradient could be a lot less; in situ instrumentation of mercury cadmium telluride ampoules has never been achieved. Breakdown was observed in the initial transient region and it is unlikely that the interface was flat. More details of this crystal are given in Section 3.3.

3.3 DIRECTIONAL SOLIDIFICATION WITH RATE CHANGES

The transient analysis model can be applied to simulate a change in translation rate during growth. Assuming a temperature gradient of 180°C/cm and $D=7\times10^{-5}cm^2/sec$ several rate changes were modeled. The translation rate of 4mm/hour was thought to be the fastest that could be used without breakdown and this was used in one simulation with a rate change to 1mm/hour after steady state had been reached. The data obtained are shown by the solid line in Figure 6. Following the rate change a new diffusion layer is set up consistent with the new translation rate. In the example shown the crystal is too short for growth to even approach steady state, end effects are observed immediately, and the composition varies continuously.

The simulation above models a real crystal grown under these

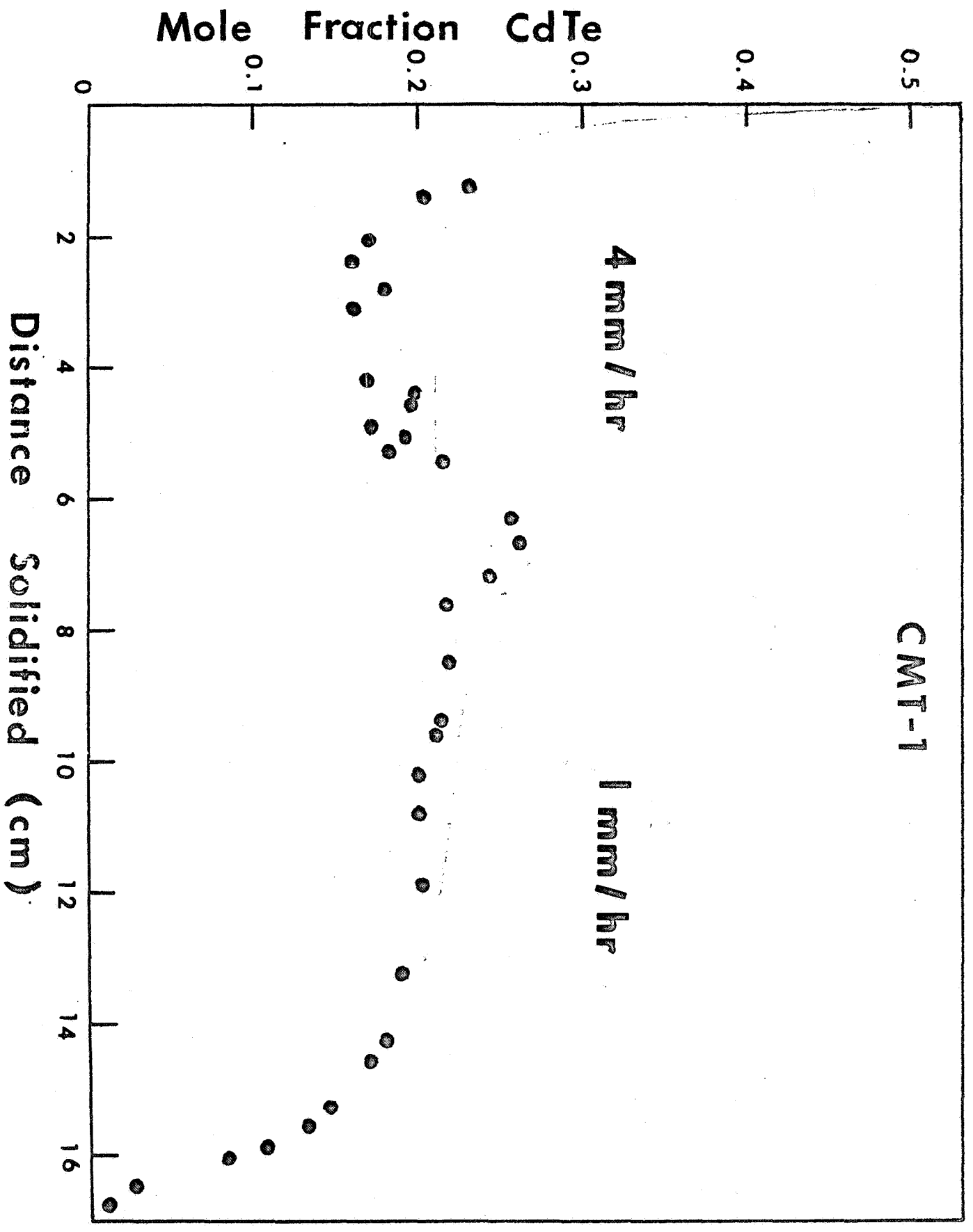

Figure 6 . Effect of Rate Change on Directional Solidification

conditions by Dr. F.R. Szofran at MDRL. The mean analysis at various locations along the length of the crystal is also shown in Figure 6. As explained in Section 3.1 a translation rate of 4mm/hour led to breakdown of the interface with a resulting dendritic structure. Concentration values varied considerably across a diameter and there is no guarantee that a valid mean value can be determined.

Nevertheless the analysis points from the real crystal do bear some resemblance to the model. Following the rate change, growth of single crystal material took place. The existence of a second initial transient is clear. As this material would be prenucleated such a region should give accurate diffusion data provided the initial growth had a more or less flat interface. Such an experiment is thus worth repeating providing the initial growth takes place under more controlled conditions.

This experiment has other implications. The determination of the shape and location of the interface is of paramount importance as a first stage of designing a controlled growth experiment. Due to the impracticability of instrumenting a mercury cadmium telluride ampoule indirect methods have to be used. The deconvolution method discussed earlier is one such method; another is the use of interface perturbation such as is present in a rate change. In principle it should be possible to determine the location in the crystal of the interface at the time the rate change occurred. At such a position there is a discontinuity in

the chemical composition caused by the setting up of a new diffusion layer. In the case of crystal CMT-1 shown in Figure 6 this determination was not attempted due to the breakdown of the interface caused by constitutional supercooling. This technique should be further investigated under more favorable experimental conditions.

3.4 INTERRUPTED GROWTH

The model can also be used to simulate behavior when translation of a crystal is stopped entirely. Under these circumstances two main changes occur assuming diffusion in the solid state can be neglected. First the liquid will homogenize reaching a composition somewhat lower in cadmium telluride than the original composition. As this liquid will no longer be in equilibrium with the solid, growth will continue and the interface will advance (toward the hot end). During this period the solid being deposited will become progressively richer in cadmium telluride until it is in equilibrium with the liquid, now homogeneous. At this moment the interface will lie along an isotherm within the furnace and an ideal situation for growth from a prenucleated crystal exists.

The model is useful here in demonstrating the lengths of ampoule needed to perform such an experiment and still achieve steady state following a re-start of growth. The length of the interruption can also be determined.

Figure 7

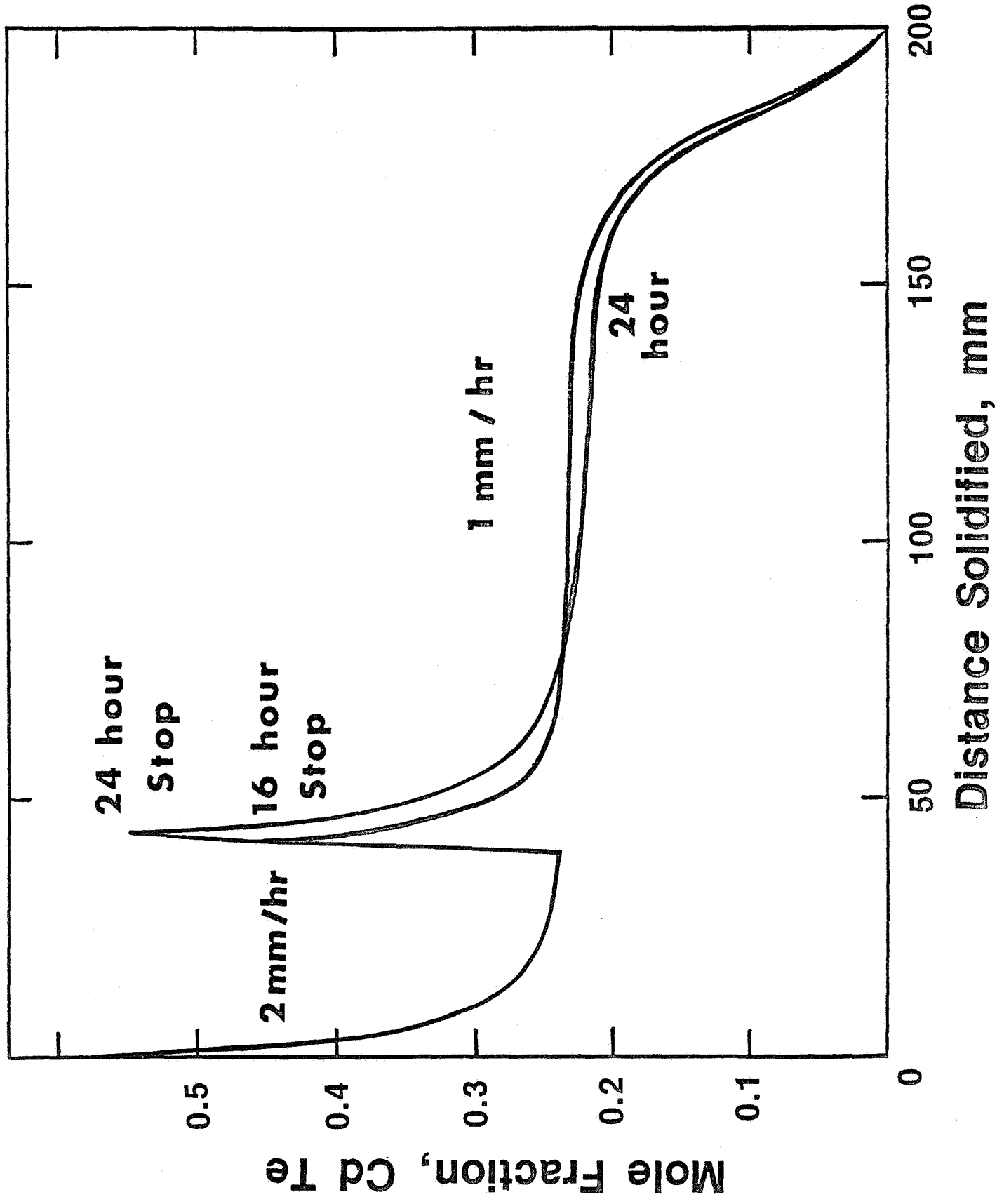
Mole Fraction, Cd Te
0.5
0.4
0.3
0.2
0.1
0
50
100
150
200
Distance Solidified, mm
2 mm/hr
1 mm / hr
24 hour Stop
16 hour Stop
24 hour

An example illustrating the method and the effect of two different stoppage times is shown in Figure 7. In this case a rate change was incorporated as well. It should be noted that the steady state region following the restart lies at a lower value than the first steady state; this is due to the incorporation of cadmium rich material in the initial transient. It is strongly recommended that a controlled experiment such as this be attempted as soon as possible. Once again, interruption of growth with or without a rate change offers a means of locating the interface due to the change in composition when growth is re-initiated.

4.0 INTERFACE DECONVOLUTION

4.1 BACKGROUND

As described in Section 2, interface evaluation is a critical factor in Bridgman Stockbarger crystal growth. The location, shape, composition, temperature and movement of the interface during the experiment are important parameters, crucial for the control and design of a successful crystal growth program. In this context mercury cadmium telluride poses its own problems. The mercury vapor pressure at the temperatures under consideration is in excess of 20 atmospheres and it has so far proved impossible to contain the material in an ampoule instrumented with feedthrough leads.

Thus the technique of Peltier pulsing which has so successfully been applied to doped germanium, and is at present being developed for lead tin telluride, cannot be used here. Any information about the interface has to be gathered either by more complex analytical techniques, such as the deconvolution method to be described, or by experimental perturbations such as the rate change described in Section 3.3. Any perturbation technique will lead only to one experimental data set for interface characterization. Any movement or change of shape of the interface during the crystal growth is difficult to ascertain in a single experiment.

This section reviews the work done so far in developing the deconvolution model, describes typical results and presents ideas

suitable for modifying the model to assist in the planning of future experiments. In another sub-section results achieved with the perturbation techniques are described and an assessment is made of their utility in future experiments.

The deconvolution technique was originally conceived by Dr. D.C. Gillies at NASA, while working as a USRA Visiting Scientist. SEMTEC has formalized the concept into a mathematically rigorous form and developed a computer program that performs the deconvolution process. The iteration technique described in the paper in the appendix is necessary to give accurate results, but the general characteristics of the process may be described below.

4.2 DECONVOLUTION - APPLICATION

The deconvolution technique effectively determines the prior locations of the liquid-solid boundary after growth is completed. For a mathematical description of the method, the reader should refer to the appendix in this report. The first attempts at seperating solidus temperatures from thermal field were made by hand using transparent paper. They serve to illustrate the method and how the computer techniques evolved from it.

A schematic representation of the procedure is shown in Figure 8a-c. Figure b is the assumed thermal field which in this case is decoupled from the crystal. The midplane is at 705°C, the solidus temperature for $Hg_{0.80}Cd_{0.20}Te$. In Figure 8 a are shown

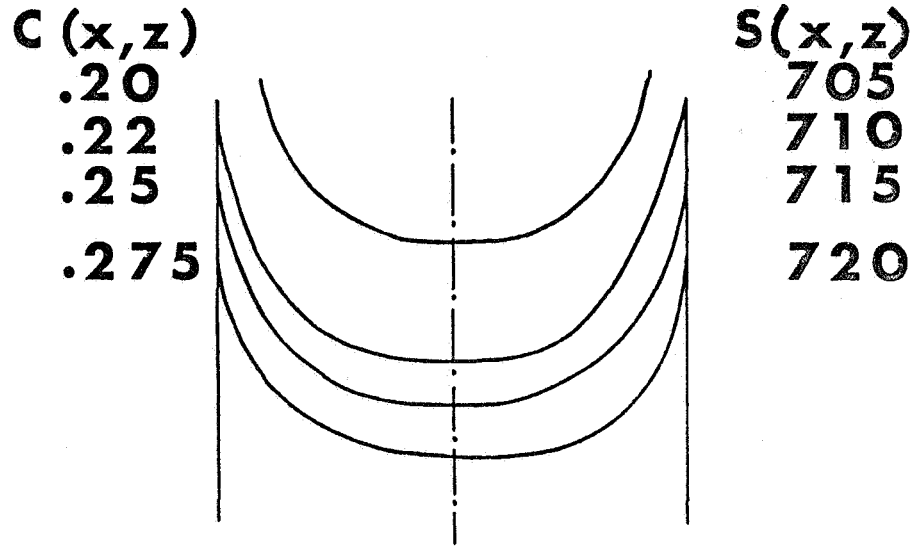

(a)

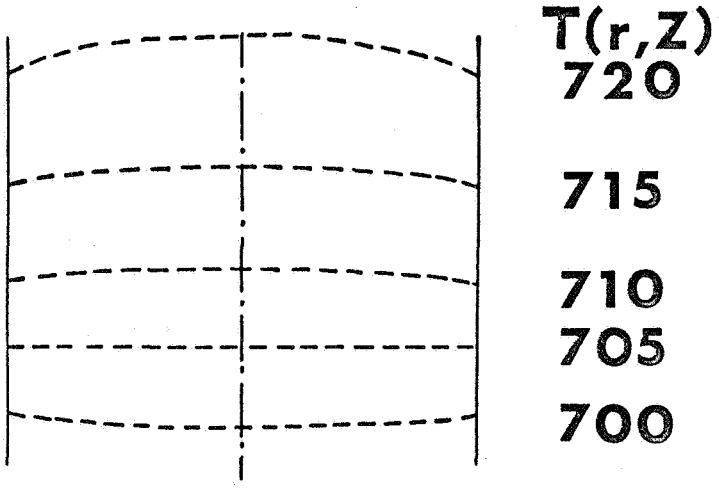

(b)

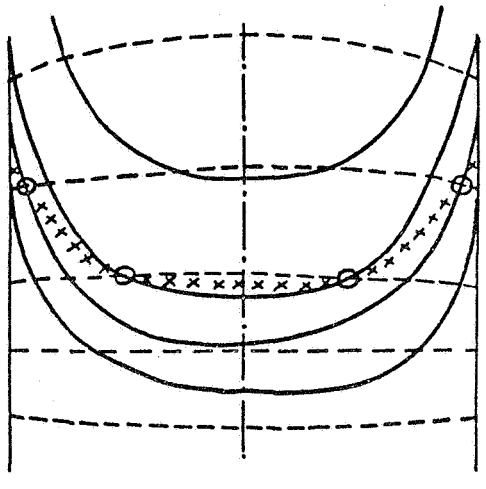

(c)

Interface ×

FIGURE 8

isoconcentration lines in the grown crystal together with their equilibrium solidus temperatures. These curves have to be constructed from the analysis data of the crystal. The superimposition of these two graphs demonstrates within the furnace frame and the crystal frame locations of the solidification front. For one instant this procedure is shown in Figure 8c. The coincidence of thermal field and solidus temperature is shown at the circles. With additional isotherms the complete interface can be reconstructed as demonstrated by the crosses. It can readily be seen that the interface is not along an isotherm nor is it an isoconcentrate. Furthermore, in this case, the interface reflects the curvature of the solidus and not that of the thermal field. The movement of Figure 8a and 8b relative to each other is a function of time and the translation rate of the ampoule or crystal. At any time a different set of coincidence points can be found corresponding to that instantaneous location of the interface. The above procedure lends itself to a computing technique; the program and its use are included as an appendix.

4.3 DECONVOLUTION - EXAMPLE

As explained previously, the complete interface deconvolution process requires iteration between the thermal model and deconvolution procedure to obtain an interface location and composition that is consistent with both the thermal boundary conditions and the measured solute profile. We may illustrate the deconvolution

procedure using composition data from an actual crystal and apply various assumed thermal fields to qualitatively describe the interface behavior.

The crystal is that used to illustrate the 1-D transient analysis model in Section 3.2. Crystal composition was $Hg_{0.80}Cd_{0.20}Te$, the diameter was 8mm, the length 21.2cm and the translation rate was 0.762mm/hour. The complete crystal analysis C(x,y) was obtained by energy dispersive spectrometry. The raw data for selected radial values of x were fitted to a polynomial, as were the thermal data, in order to implement the deconvolution procedure. C(x,y) values were converted to S(x,y), the corresponding equilibrium solidus temperatures by the deconvolution computer program. It is S(x,y) that has been plotted in Figure 9 to illustrate compositional variations throughout the crystal. This crystal was not grown under ideal conditions; there is a pronounced asymmetry and a pronounced drop in the isoconcentration lines close to the right hand edge.

Of significance is that the isoconcentration lines are extremely curved even towards the top of the illustrated section which lies close to the steady state region. If the interface were an isoconcentrate its curvature would have to be extreme. It is conceivable that the thermal field is distorted to the extent that solidification along an isotherm could yield the isoconcentrate shapes presented in Figure 9; however, we will see

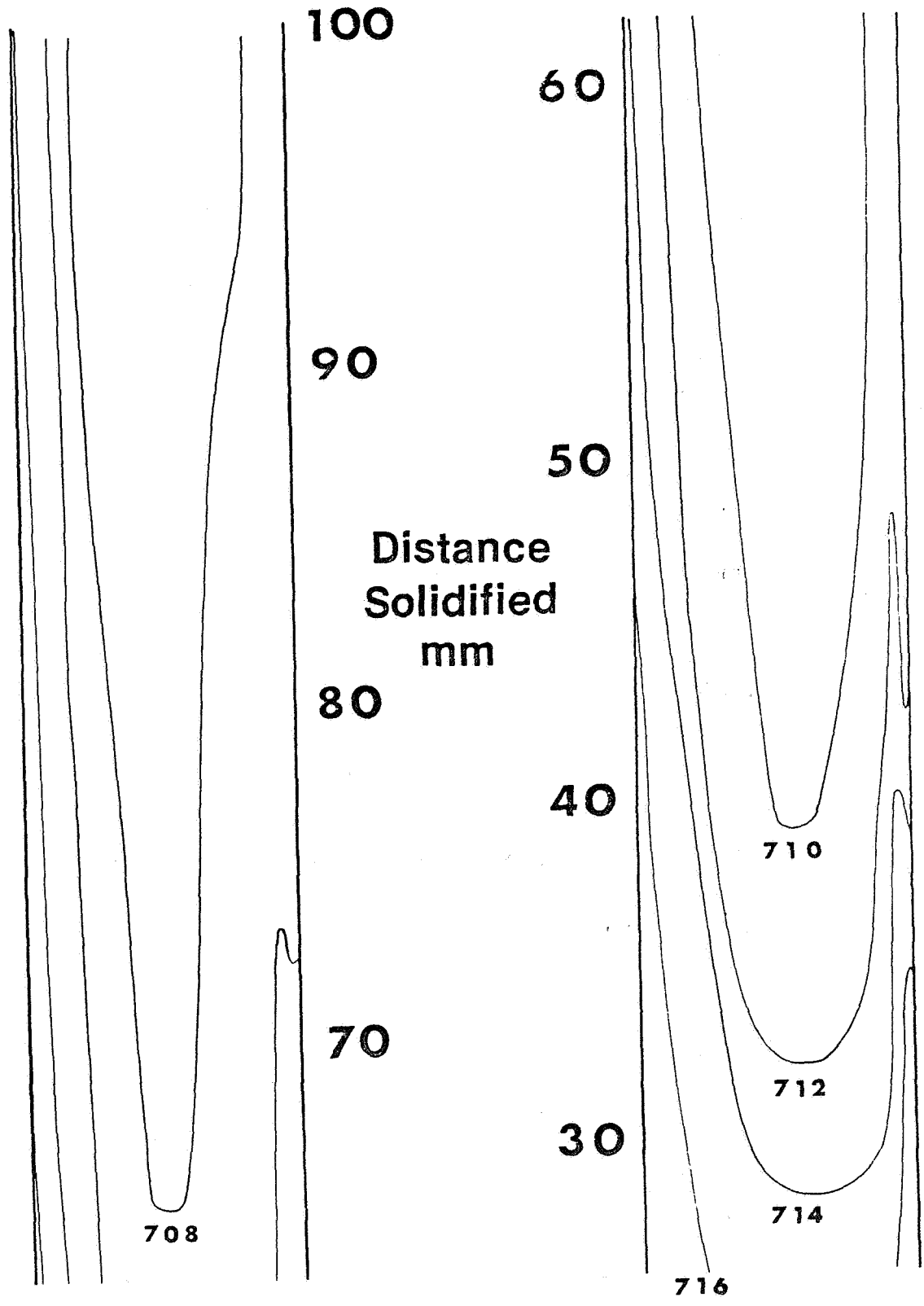
100
90
80
70
60
50
40
30
Distance
Solidified
mm
708
710
712
714
716

Figure 9

that postulating a more reasonable thermal field leads to an interface of moderate curvature consistent with the composition data.

Two thermal fields were chosen to illustrate the application of the method. The two fields are shown in Figure 10. Each has one flat isotherm and a temperature gradient of 200°C/cm along the centerline of the furnace. In one case the flat isotherm is at 700°C and in the other at 750°C. These two values were chosen as extremes. In thermal field 1 (700°C flat isotherm) solidification would take place above the flat isotherm in a region where the isotherms are convex (i.e. directed upward at the center). Conversely in thermal field 2 the isotherms are in the opposite direction.

The "deconvolution" will give resulting interface shapes, locations and temperature anywhere within the range of the calculated polynomials for S(C(x,y)) and T(x,y). Figure 11 shows the interface for both thermal fields at two selected points in the crystal and thus at two different times during growth, measured in the furnace frame. The temperatures and actual locations are given in Table 1. The interface at the same time for thermal field 2 is also shown in Figure 11 and in Table 2. It can be seen that in both cases the interface was concave (i.e. directed downward at the center), but the degree of curvature is very dependent on the isotherm curvature within the region of solidification. Thermal field 1 has convex isotherms at the solidification temperature

Figure 10

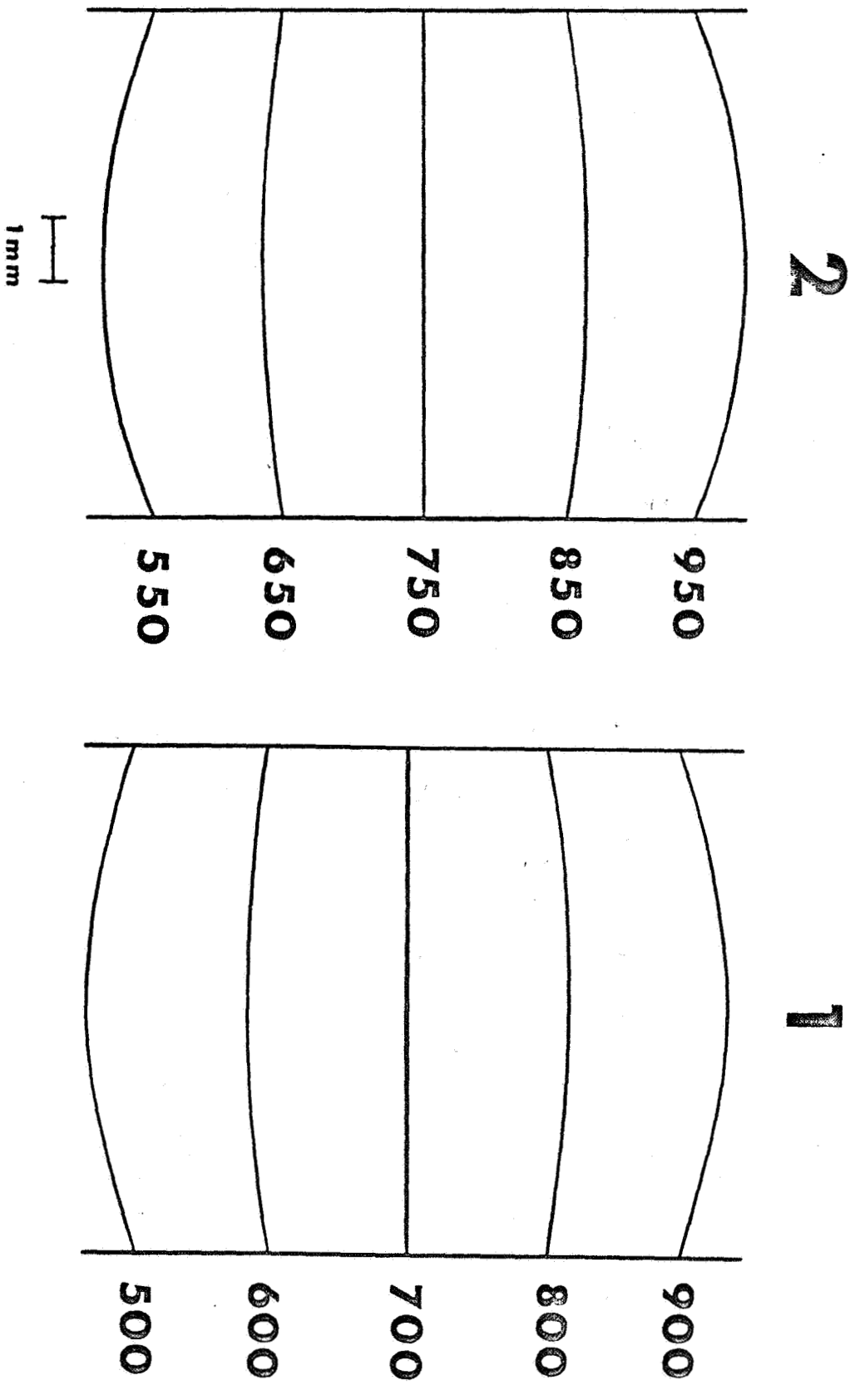

Figure 11

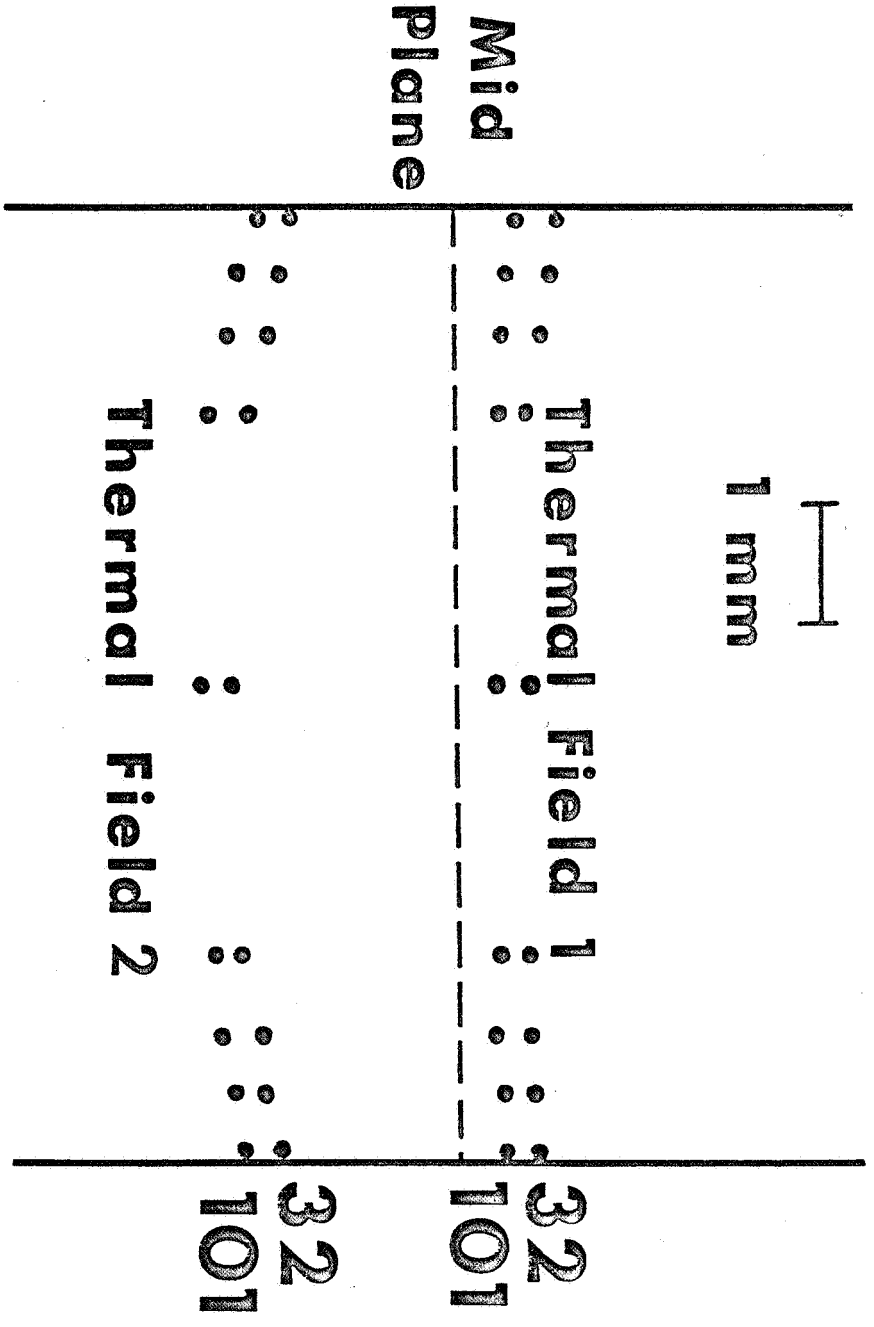

TABLE 1

RESULTS OF DECONVOLUTION USING THERMAL FIELD 1

	x, mm	Temperature, °C	y, mm	y**, mm
Time* 1 Hour	-3.916	721.9	26.01	0.96
	-3.440	720.6	25.97	0.93
	-2.919	718.6	25.90	0.86
	-2.252	716.1	25.82	0.78
	0	714.2	25.75	0.71
	2.252	714.6	25.75	0.71
	2.919	714.8	25.72	0.69
	3.440	715.8	25.76	0.72
	3.916	718.5	25.86	0.82
Time 10 Hours	-3.916	719.1	32.72	0.84
	-3.440	717.7	32.68	0.80
	-2.919	716.1	32.63	0.74
	-2.252	713.9	32.55	0.67
	0	712.4	32.02	0.62
	2.252	712.2	32.47	0.59
	2.919	713.3	32.50	0.61
	3.440	713.6	32.50	0.62
	3.916	715.8	32.58	0.70
Time 100 Hours	-3.916	711.6	100.79	0.51
	-3.440	710.2	100.75	0.46
	-2.919	708.9	100.69	0.41
	-2.252	707.8	100.66	0.38
	0	706.4	100.60	0.32
	2.252	707.8	100.66	0.38
	2.919	706.6	100.58	0.30
	3.440	708.6	100.67	0.39
	3.916	709.1	100.68	0.40

* Time taken assuming T = 0 for distance solidified = 25mm

** y = location with respect to mid-plane

TABLE 2

RESULTS OF DECONVOLUTION USING THERMAL FIELD 2

	x ,mm	Temperature,°C	y ,mm	y^{**} ,mm
Time	-3.916	721.8	26.15	-1.24
1 Hour	-3.440	720.5	26.05	-1.34
	-2.919	718.5	25.94	-1.45
	-2.252	716.0	25.75	-1.64
	0	714.8	25.74	-1.76
	2.252	714.5	25.78	-1.71
	2.919	714.8	25.88	-1.62
	3.440	715.7	25.94	-1.56
	3.916	718.3	26.11	-1.39
Time	-3.916	719.2	32.87	-1.34
10 Hours	-3.440	717.6	32.77	-1.47
	-2.919	716.2	32.67	-1.56
	-2.252	714.0	32.49	-1.74
	0	711.9	32.43	-1.91
	2.252	712.2	32.51	-1.82
	2.919	713.3	32.65	-1.69
	3.440	713.5	32.68	-1.65
	3.916	718.9	32.84	-1.50
Time	-3.916	711.7	101.06	-1.68
100 Hours	-3.440	710.2	100.93	-1.81
	-2.919	709.0	100.85	-1.89
	-2.252	707.9	100.71	-2.03
	0	706.2	100.55	-2.19
	2.252	707.9	100.70	-2.03
	2.919	706.6	100.74	-2.00
	3.440	708.6	100.86	-1.89
	3.916	709.2	100.95	-1.79

yet the interface is concave. For thermal field 2 the convex isotherms lead to a much more pronounced concave curvature in the interface.

We also note from Tables 1 and 2 that the interface curvature changes slightly as solidification proceeds along the crystal. There is some scatter in the data due to the asymmetry of the compositional analysis and the drop in concentration occurring at the right hand side (positive x values) as seen in Figure 9. The important point is that in both cases the interface curvature is concave and is far less curved than what would be expected from the curvature of the isoconcentration lines. The interface does not follow the curvature of the isotherms as indicated by a concave interface consistent with convex isotherms in thermal field 1. This example indicates the importance of interface curvature on solute redistribution. A complete analysis using iteration between a thermal model and analyzed data is necessary to determine the actual degree of interface curvature encountered in HgCdTe growth experiments.

5.0 TWO DIMENSIONAL SEGREGATION

5.1 BACKGROUND

The results of crystal growth of HgCdTe shown in the previous chapters have illustrated some of the problems associated with the growth of this material. While longitudinal segregation would be expected as a natural result of directional solidification of a solid solution material, there is no obvious and simple explanation for the observed radial segregation.

As has been discussed earlier, the problem can be considered in two parts. The first part is concerned with diffusion in 2-Dimensions and will attempt to elucidate some of the work of other researchers and apply their results to HgCdTe. The second part is concerned with developing and demonstrating some of the equations and data for determining the effects of fluid flow and assessing the possible effects of "Shape Instability".

5.2 TWO - DIMENSIONAL DIFFUSION

Lateral solution segregation has been the subject of recent papers [2, 3] and it was felt that it should be carefully appraised to determine its applicability to HgCdTe. The interface composition, and shape as determined by the deconvolution analysis described in the previous chapter can be incorporated in the model of Coriell et al (3).They examined the unidirectional solidification behavior of a solid solution material with a curved liquid-solid

interface. The nomenclature, including figures, tables, symbols and equations is identical to those in their publication.

Let V=velocity of solidification in +y" direction

L=diameter of ampoule

D=Diffusion Coefficient in liquid (D=0 in solid)

x'=direction perpendicular to growth direction.

Ampoule walls are at $x' = \pm L/2$

Shape of the liquid/solid interface is given by:

$$y' = W'(x') \tag{5.1}$$

Introduce the dimensionless parameters

$$x = x'/L;\ y=y'/L,\ \beta=VL/D \text{ and } C=C'/C'_{\infty} \tag{5.2}$$

The relevant equations can be written as:

$$\nabla^2 C+\beta(\partial C/\partial y) = 0 \tag{5.3}$$

$$\beta C_I(k-1) = (\partial C/\partial y)_I - (\partial C/\partial x)_I\ (\partial W/\partial x) \tag{5.4}$$

$$C(x,y\to\infty) = 1 \tag{5.5}$$

$$\frac{\partial C}{\partial x} = 0 \text{ at } x = \pm \tfrac{1}{2}. \tag{5.6}$$

C' is the concentration of solute in the liquid at the interface and C'_{∞} is the bulk solute concentration. Subscript I refers to the interface.

Coriell et al. assumed the interface shape to satisfy the equation $W(x) = \delta\cos(2\pi x)$, where δ is the amplitude across the diameter. This presents a problem in comparing our data to Coriell's results in that the interface shapes we observe and

obtain from the deconvolution process are concave to the liquid, and the expression used by Coriell results in a convex interface for positive values of δ . Due to the boundary condition at the ampoule wall, these two interface shapes may lead to different values in the change in solute concentration across the interface for the same deviation from planarity of the interface. It is instructive, however, to compare results for the same absolute values of deviations in composition and deviations from planarity for our concave interfaces and Coriell's result for a convex interface. Further work should be done to obtain results for the same sense of interface curvature. With this restriction in mind, we may compare results using Coriell's tabulated results in their paper in Table 1 and their Figures 2-8.

The crystal described in section 4 was chosen for comparison. The pull rate was 0.0762cm/hr with a diameter of 0.8cm. Assuming an effective diffusion constant of $7\times10^{-5}\text{cm}^2/\text{sec}$ we have

$$\beta/4\pi = \frac{0.0762 \times .8}{7\times10^{-5}\times3600\times4\pi} = 0.019, \tag{5.7}$$

and we take $C'_\infty = .2$ and $k=4$.

Coriell et al's results correlate δ, the interface amplitude over a diameter, to the concentration at the interface center and edge ($C_{SI}(0)$ and $C_{SI}(\frac{1}{2})$) respectively.

Table 1 in Coriell's paper includes values calculated for k=0.4, k=2, and k=10. These were plotted and values for k=4 interpolated as follows;

k	$\beta/4\pi$	δ	$C_{SI}(0)$	$C_{SI}(\frac{1}{2})$
4	.01	0.1	1.037	0.965
4	.1	0.1	1.180	0.745

Note that the solute concentration at the center of the interface, $C_{SI}(0)$, is higher than that at the edge. This is due to the assumption of a convex interface. A concave interface will yield solute concentrations that are higher at the edges than at the center. As discussed before we will compare the magnitude of the concentration change to the magnitude of the deviation from planarity, although this comparison between concave and convex interface shapes may not be valid for larger deviations from planarity.

Further interpolation was used to estimate values for $\beta/4=0.019$.

k	$\beta/4\pi$	δ	$C_{SI}(0)$	$C_{SI}(\frac{1}{2})$	ΔC_{SI}
4	0.019	.1	1.05	0.94	0.11

The crystal considered in section 4 with the concentration profiles given in Figure 9 gives the following normalized con-

centration differences for an interface shape deconvoluted using thermal field 1 (see Table 1 in section 4).

$$C_{SI}(0) = 1$$

$$C_{SI}(-\tfrac{1}{2}) = 1.14 \qquad \delta = \frac{.19}{8x2} = 0.012$$

$$C_{SI}(+\tfrac{1}{2}) = 1.075 \qquad \delta = \frac{.08}{8x2} = .005$$

We see that even though the measured interface from section 4 is asymmetric, we find ΔC_{SI} values between .075 and .14 corresponding to δ values between .005 and .012. Based on solute transport by diffusion, Coriells results indicate that a ΔC_{SI}=.11, intermediate to our results, corresponds to an interface amplitude of δ =.1, which is an order of magnitude higher than that obtained from the interface deconvoluted in section 4. Although this comparison is quite tenuous due to the number of assumptions made, we may make the following observations.

Let us consider the maximum possible deviation from planarity for the interface. We argue as follows. For k>1, solute (CdTe) is preferentially incorporated from a bulk liquid of concentration C_o at steady state. For a concave interface, the solute concentration will be highest at the edges and lowest at the center for either diffusion or shape instability. The minimum solute concentration possible in the liquid is obviously zero and the maximum possible liquid concentration is C_o. Thus the maximum solute differential across the interface by any mechanism is $(C_o-0)=C_o$, and

thus the solid concentration difference is k C_o at a maximum. HgCdTe liquid of concentration C_o freezes at 805°C, and pure HgTe (C=0) feeezes at 668°C, a temperature difference of 137°C. Under this extreme example, the center of the interface lies at a point 137°C cooler than the edge. If all isotherms were planar, this would correspond to a center to edge deviation from planarity of.68cm in a 200°C/cm gradient. Note that this is not necessarily the maximum interface curvature since we are stating that the interface edge lies 137°C off of the 668°C isotherm, curvature of the isotherms may result in interface displacements more or less than given by planar isotherms.

The concentration data for the crystal analyzed in our table 1, section 4, gave values for the solid concentration at the center of approximately $C_s(0)=.2$ and at the edge $C_s(-\frac{1}{2})=.228$, corresponding to a solidus temperature difference of about 5°C. This indicates that the maximum deviation of the interface from an isotherm for a gradient of 200°C/cm is 0.25mm (5°C/200°C/cm). The observed interface curvature may be more or less than this due to curvature of the isotherms. Consider a constant gradient of 200°C throughout the solidification region. If the interface lies in a region of convex isotherms (as in thermal field 1, section 4) but remains concave, a temperature difference between the sample center and edge of 5°C will result in an interface curvature of less than 0.25mm. On the other hand, if the interface is convex, its deviation from planarity will be 0.25mm less than that of the isotherms. In a region of concave isotherms the deviation from planarity will be 0.25mm greater than the isotherms and the interface will be concave.

Returning to Coriell's results we find that to obtain a concentration difference of the order of $\Delta C_{SI}/C_o = .11$, we must have a $\delta = .1$, which for an 8mm diameter ampoule used in the crystal discussed results in an interface deviation of 1.6mm. Although such deviations are possible for this crystal, the interface would have to have been located in the cold zone with concave isotherms. The isotherms would have to be curved such that the center of the isotherm lay 1.6mm-.25mm$\sim$1.4mm below the same isotherm at the sample edge. Once again, this is a possibility, thus more accurate measurements and improved thermal models must be used to ascertain whether lateral diffusion alone can account for the radial solute distribution. We may state that for the reasonable thermal fields assumed here, the interface curvature is far too little to yield the observed solute distribution due to diffusion alone.

Since solution of the two dimensional diffusion problem is of major importance in determining the cause of radial solute profiles, SEMTEC has developed its own two dimensional diffusion model to calculate interface concentration for an assumed interface shape. We see to solve the same problem as Coriell et al (2), namely

$$\nabla^2 C + (V/D) \frac{\partial C}{\partial y} = 0 \qquad (5.8)$$

where C is the liquid solute concentration, V the translation

rate, and D the diffusion constant in the liquid. The coordinates x,y are centered at the sample mid-line with y positive into the liquid and the sample walls are at x=±a. The boundary conditions are

$$V(k-1)C_I = D[(\partial C/\partial y)_I - (\partial C/\partial x)_I(\partial W/\partial x)], \tag{5.9}$$

$$C(y\to\infty) = C_o, \tag{5.10}$$

and $$\partial C/\partial x = 0 \quad \text{at } x=\pm a. \tag{5.11}$$

Here I denotes evaluation at the solid-liquid interface and the interface shape is assumed to be y=W(x).

Since this is a time independent problem, we may write equation 5.9 in a central finite difference form appropriate for numerical calculations. Let C_{ij} denote a point in the liquid not on the interface. Define

$$\begin{aligned} h_1 &= x_i - x_{i-1} \\ h_2 &= x_{i+1} - x_i \\ g_1 &= y_j - y_{j-1} \\ g_2 &= y_{j+1} - y_j \end{aligned} \tag{5.12}$$

as the internodal distances from node (i,j) to its neighboring

nodes. After much algebra we obtain the finite difference form of equation 5.8 as

$$C_{ij} = \frac{1}{p} \left[C_{i+1,j}Q + C_{i-1,j}\ R+C_{i,j+1}S+C_{i,j-1}T\right] \qquad (5.13)$$

with

$$P = 4/H^2 + 4/G^2 - 2(h_2-h_1)(h_1^2 - h_2^2)/(AH^2) \qquad (5.14)$$

$$-2(g_2-g_1)(g_1^2 -g_2^2)/(G^2\ B) + V(g_1^2 -g_2^2)/(BD)$$

$$Q=2/H^2 - 2h_1^2\ (h_2-h_1)/(AH^2) \qquad (5.15)$$

$$R=2/H^2 + 2h_2^2\ (h_2-h_1)/(AH^2) \qquad (5.16)$$

$$S=2/G^2 - 2g_1^2\ (g_2-g_1)/(BG^2)+Vg_1^2(BD) \qquad (5.17)$$

$$T=2/G^2 + 2g_1^2\ (g_2-g_1)/(BG^2) - Vg_2^2\ /(BD) \qquad (5.18)$$

with

$$H^2 = h_1^2 + h_2^2 \qquad (5.19)$$

$$G^2 = g_1^2 + g_2^2 \qquad (5.20)$$

$$A = h_1^2h_2+h_2^2h_1 \qquad (5.21)$$

$$B = g_1^2g_2+g_2^2g_1 \qquad (5.22)$$

This rather complicated form allows variable node spacing in all directions to allow for chosing a node structure that gives the most accurate results.

The boundary condition at the interface creates a problem in that solute concentrations are only defined for points on and in the liquid side of the interface. A central difference formalism is inappropriate here and we must write equations specific to either a concave or convex interface. Choosing a concave interface, we must use the backward difference form for $(\partial c/\partial x)_I$, and the forward difference form for $(\partial C/\partial y)_I$.

Label the interface points by the index m and consider points along the interface with the same x values as chosen for nodes in the liquid. If the liquid nodal points are at x_i, y_j then the interface points are at X_i, Y_j where $X_i = x_i$ and $Y_j = W(x_i)$. Define

Cm = concentration of m-th point on interface, coordinates $(x_m, W(x_m))$.

CA = concentration of point in liquid above point on interface. Coordinate is (x_m, y_{j+1}) where $y_{j+1} \geq W(x_m) \geq y_j$.

CL = concentration of point in liquid at $(x_{m-1}, W(x_m))$, i.e. to the left of the interface point for a concave interface. This value must be interpolated from concentration at

the nodes $y_{j+1} \geq W(x_m) \geq y_j$.

We may write

$$\left.\frac{\partial C}{\partial y}\right)_I = (CA-Cm)/(y_j-Y_j), \tag{5.23}$$

$$\partial C/\partial x)_I = (Cm-CL)/(x_m-x_{m-1}), \tag{5.24}$$

This gives the finite difference form of the boundary condition in equation 5.9 as

$$C_m = \frac{1}{u}\left[CA/(y_j-Y_j)+CL(\partial W/\partial x)/(x_m-x_{m-1})\right] \tag{5.25}$$

with $$u = V(k-1)/D+1/y_j-Y_j)+(\partial W/\partial x)/(x_m-x_{m-1}). \tag{5.26}$$

Equations 5.13 and 5.26 form the basis for a finite difference method of solution of the two dimensional diffusion problem. Programming of these equations together with treatment of the sample edge and sample end boundary conditions has been underway. The total program is to date incomplete due to changes in the method of treating the interface nodes. Completion of the program for two dimensional diffusion will be carried out early in the next years effort.

5.3 SHAPE INSTABILITY

The phenomenon of shape instability has been qualitatively described in a previous section of this report. In this section an attempt is made to formulate this instability. No attempt is made to describe the most general problem, the interest being more in demonstrating the general characteristics and more importantly providing a theoretical basis for experimentation. Thus several simplifying assumptions are made while retaining the general character of the problem. As a first step we assume the following.

A. The fluid motion is incompressible, that is the fluid density is not a function of the pressure (P).

B. The fluid density is a linear function of temperature (T) and concentration (C).

C. Heat transport by fluid motion is ignored.

D. The dynamic viscosity ν, the thermal conductivity k_T and the specific heats are constant.

These assumptions define the so called simplified Oberbeck-Boussinesq problem. If in addition the stress in the momentum balance is ignored, we may write the following equations.

$$\frac{\partial T}{\partial t} + \bar{u}\cdot\nabla T=\kappa_T\nabla^2 T, \tag{5.27A}$$

$$\frac{\partial C}{\partial t} + \bar{u}\cdot \nabla C=D\nabla^2 C, \tag{5.27B}$$

$$\frac{\partial \bar{u}}{\partial t} + (\bar{u}\cdot\nabla)\bar{u} = - 1/\rho_o \nabla P+\nu\nabla^2\bar{u} + \bar{g}\ (\rho/\rho_o-1), \tag{5.27C}$$

$$\bar{\nabla}\cdot\bar{u} = 0 \tag{5.27D}$$

with the constitutive relations

$$\rho= \rho_o\ [1-\alpha(T-T_o) - \beta(C-C_o)], \tag{5.27E}$$

$$C(y\to\infty) = C_o, \tag{5.27F}$$

$$C_{SI}=k\ C_I \tag{5.27G}$$

$$T_e=T_m+m_1C_I+m_2C_I^2 \tag{5.27H}$$

Here κ_T is the thermal diffusivity, $\bar{u}$ the fluid velocity, ν the kinematic viscosity, P a pressure, $\bar{g}$ the gravity vector, and C the solute (CdTe) concentration in the liquid. Equation (5.27E) relates the fluid density ρ to the temperature and concentration and equation (5.27H)

approximates the interface temperature as a function of composition C_I. The coordinate system (x,y,z) is an inertial frame fixed to the ampoule tip with the y-axis along the sample axis positive into the liquid. The boundary conditions for the thermal field T are usually specified in a laboratory (furnace fixed) frame which moves with some pull rate R with respect to the ampoule.

We now transform these equations into a coordinate system fixed to the center of the solid-liquid interface which moves with a velocity v_o. Let the coordinates be (ξ,η,ζ) with η positive into the liquid. Denote the transformed fluid velocity as $\bar{\sigma}\ (\xi,\eta,\zeta)$, and the solute concentration as $\gamma(\xi,\eta,\zeta) = C(x,y,z)$.

The transformed equations become

$$\frac{\partial \gamma}{\partial t} + \bar{\sigma}\cdot\nabla\gamma = D\nabla^2\gamma \ , \tag{5.28A}$$

$$\frac{\partial \bar{\sigma}}{\partial t} - \dot{\bar{v}}_o + (\bar{\sigma}\cdot\bar{\nabla})\bar{\sigma} = -1/\rho_o \ \nabla P' + \nu\nabla^2\bar{\sigma} + \bar{g}\ (\rho/\rho_o - 1), \tag{5.28B}$$

$$\bar{\nabla}\cdot\bar{\sigma} = 0, \tag{5.28C}$$

$$\rho = \rho_o[1-\alpha(T-T_o) - \beta(\gamma-\gamma_o)\ ], \tag{5.28D}$$

$$\gamma(\eta\to\infty) = \gamma_o, \tag{5.28E}$$

$$\gamma_{SI} = k\ \gamma_I, \tag{5.28F}$$

$$T_e = T_m + m_1 \gamma_I + m_2 \gamma_I^2 . \qquad (5.28G)$$

Note that the only change is that we pick up an additional acceleration term in equation (5.28B). We have temporarily ignored the thermal field and will express it in the original coordinate system. The boundary condition at the solid-liquid interface is

$$\bar{v} \cdot \bar{n} \quad (\gamma_{SI} - \gamma_I) = D \bar{\nabla} \gamma \cdot \bar{n} , \qquad (5.28H)$$

where $\bar{v}$ is the actual growth velocity and $\bar{n}$ the unit normal to the interface. We have not assumed a planar interface, but rather have moved into a frame attached to the center of the interface (assumed symmetric) whose velocity is v. Thus $v=v_o$ at the center of the interface but not necessarily at other points along the interface.

Equations (5.28A) through (5.28H), together with the thermal field equation provide the general basis for the study of shape instability. Initially we will decouple the thermal field by assuming a linear thermal field with flat isotherms in order to demonstrate the essential behavior of these equations. Later in the analysis we may reintroduce the thermal field equation or arrive at the thermal field by using a thermal model and interface deconvolution.

The first step in investigating the nature of shape instability is to assume that there exists a steady state such that $\frac{\partial \bar{\sigma}}{\partial t}$ and $\frac{\partial \gamma}{\partial t}$ vanish. The existence of such a steady state has not been proven experimentally, however there is no reason to assume a priori that the features of shape instability would violate such an assumption. Further simplification of the equations can be made by making assumptions about the nature of the fluid flow due to shape instability. We must exercise caution to avoid "throwing away" terms that are essential to the overall process of shape instability. The reduced set of equations can then be used to assess the influence of gravity and thermal field on interface shape.

The full set of equations under steady state conditions may be solved numerically given the proper boundary conditions. Note that we are interested in a solution of the equations involving macroscopic deviations of the interface from planarity under conditions that would normally lead to a thermosolutally stable configuration, i.e., hot end up and increasing density downward with respect to gravity. This situation and the resulting interface shape instability have not been addressed by other workers investigating convective instabilities or interfacial instabilities. Conclusive theoretical evidence for shape instability will be a prime justification for solid solution crystal growth in a microgravity environment.

We may derive a generalized relation for the mass balance along the interface. We assume that a steady-state exist such that $\frac{\partial \gamma}{\partial t}$ and $\frac{\partial \bar{\sigma}}{\partial t}$ vanish. Furthermore we assume that in the steady-state the interface shape remains constant and thus the growth velocity $\bar{v} = v_o \hat{\eta}$ and that the ampoule is sufficiently long such that there exist an η_∞ so that $\gamma \to \gamma_o, \frac{\partial \gamma}{\partial \eta} \to 0$, and there is no fluid motion due to convection as $\eta \to \eta_\infty$. Consider the following relations from the set of equations described earlier.

$$\bar{\nabla} \cdot \bar{\sigma} = 0 \tag{5.29}$$

$$\bar{\sigma} \cdot \bar{\nabla} \gamma = D \nabla^2 \gamma \tag{5.30}$$

and

$$\bar{v} \cdot \hat{n} (k-1) \gamma_I = D \bar{\nabla} \gamma \cdot \hat{n} \tag{5.31}$$

If the interface is denoted by

$$\eta = W(\xi) \tag{5.32}$$

then the unit normal to the interface is given by

$$\hat{n} = B(\hat{\eta} - (\partial W / \partial \xi)\, \hat{\xi}) \tag{5.33}$$

where

$$B = (1 + (\partial W / \partial \xi)^2)^{-\frac{1}{2}} \tag{5.34}$$

writing

$$\bar{\sigma} = \sigma_1 \hat{\xi} + \sigma_2 \hat{\eta} \tag{5.35}$$

then equation (5.30) becomes

$$D[\partial^2\gamma/\partial\xi^2 + \partial^2\gamma/\partial\eta^2] = \sigma_1(\partial\gamma/\partial\xi) + \sigma_2(\partial\gamma/\partial\eta) \tag{5.36}$$

This may be written in a different form as

$$\begin{aligned} &\partial/\partial\xi(\partial\gamma/\partial\xi - \sigma_1\gamma/D) + \frac{\partial}{\partial\eta}(\partial\gamma/\partial\eta - \sigma_2\gamma/D) \\ &+(\gamma/D)(\partial\sigma_1/\partial\xi + \partial\sigma_2/\partial\eta) = 0. \end{aligned} \tag{5.37}$$

Note that the boundary condition in equation (5.29) gives

$$\partial\sigma_1/\partial\xi + \partial\sigma_2/\partial\eta = 0, \tag{5.38}$$

thus equation (5.37) reduces to the form

$$\partial N/\partial\xi - \partial M/\partial\eta = 0 \tag{5.39}$$

with

$$N = \partial\gamma/\partial\xi - \sigma_1\gamma/D \tag{5.40}$$

$$M = -(\partial\gamma/\partial\eta - \sigma_2\gamma/D). \tag{5.41}$$

Now Gauss' theorem is of the form

$$\iint_R (\partial N/\partial \xi - \partial M/\partial \eta)\, d\eta d\xi = \oint_C M d\xi + N d\eta \qquad (5.42)$$

for a region R bounded by a closed path C. Integretion of eqn. (5.39) and application of Gauss' theorem gives

$$\oint_C -(\partial \gamma/\partial \eta - \sigma_2 \gamma/D) d\xi + (\partial \gamma/\partial \xi - \sigma_1 \gamma/D) d\eta = 0 \qquad (5.43)$$

Consider the sketch below representing a sample, interface and the liquid region bounded by an ampoule at $\eta = \pm a$.

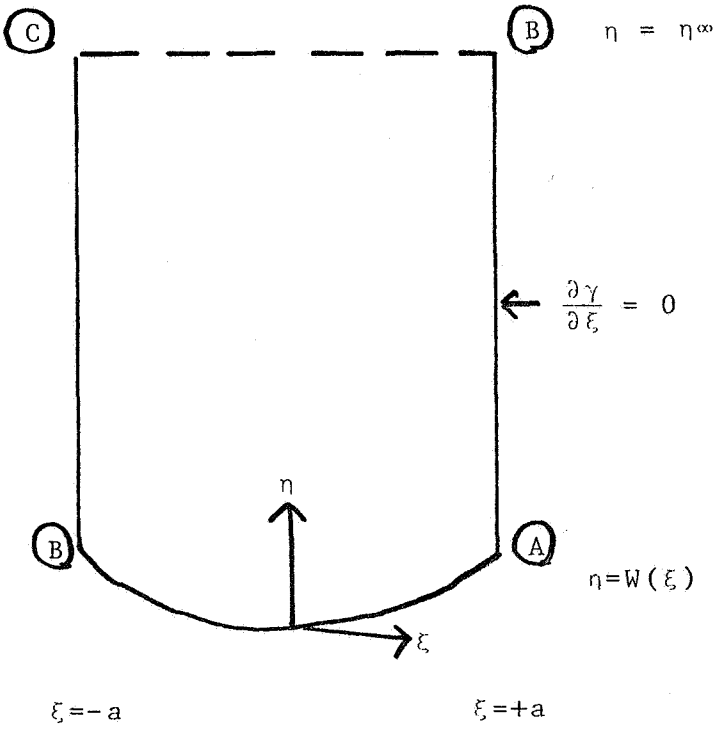

We wish to evaluate equation (5.43) along the closed path A-B-C-D-A. Write the integral as a series of line integrals

$$\oint_C = \int_A^B + \int_B^C + \int_C^D + \int_D^A = 0.$$

We note that along A-B we have the following

$$\zeta = a, \quad d\xi = 0, \frac{\partial \gamma}{\partial \xi} = 0, \sigma_1 = 0$$

and thus

$$\int_A^B = 0 \ . \tag{5.44}$$

In a similar manner we note that

$$\int_C^D = 0. \tag{5.45}$$

Evaluation of the path integral along B-C we note that

$$\eta = \eta_\infty, \quad d\eta = 0, \sigma_1 = 0, \sigma_2 = -v_o$$

giving

$$\int_B^C = \int_a^{-a} -(\partial\gamma/\partial\eta) v_o \gamma/D) \, d\xi \Big|_{\eta=\eta_\infty} \tag{5.46}$$

As $\eta\to\infty$ we have $\frac{\partial\gamma}{\partial\eta}\to 0$ and $\gamma \to \gamma_o$ so that we obtain

$$\int_B^C = 2a\, v_o\gamma_o/D \text{ as } \eta\to\infty \tag{5.47}$$

The final path integral is along the interface from D-A. Here we have

$$\eta=W(\xi),\ d\eta=\frac{\partial W}{\partial\xi}\,d\xi \quad \text{giving}$$

$$\int_D^A = \int_{-a}^{a}((\gamma/D)(\sigma_2-\sigma_1\ \partial W/\partial\xi)+(\partial\gamma/\partial\xi)(\partial W/\partial\xi)-\partial\gamma/\partial\eta)\,d\xi \tag{5.48}$$

where all quantities are evaluated along the interface.

Combining all the path integrals gives

$$\int_{-a}^{a}[\gamma(\sigma_2-\sigma_1\partial W/\partial\xi)+D((\partial\gamma/\partial\xi)(\partial W/\partial\xi)-\partial\gamma/\partial\eta)]\,d\xi=-2av_o\gamma_o \tag{5.49}$$

Now we use the boundary equation at the interface, equation (5.31) to write

$$(k-1)\ v_o\gamma_I = D[(\partial\gamma/\partial\xi)(\partial W/\partial\xi)-\partial\gamma/\partial\eta] \tag{5.50}$$

where we have taken $\bar{v} = v_o \eta$. Equation (5.49) then becomes

$$\int_{-a}^{a} \gamma_I \left(\sigma_2 - \sigma_1 (\partial W/\partial \xi) - (k-1)\, v_o\right)_I d\xi = -2a\, {}_o\gamma_o \qquad (5.51)$$

This is the generalized solute balance equation where all quantities are evaluated along the interface. It relates the net solute balance due to segregation, motion of the interface, and fluid flow to the solute in the bulk liquid γ_o. The equation (5.51) reduces to a more familiar form if we assume that the only fluid motion is that due to advancement of the interface (remember that $\bar{\sigma}$ is the fluid velocity measured in the interface fixed coordinate system). For this case we have

$$\sigma_1 = 0, \quad \sigma_2 = -v_o \qquad \text{giving}$$

$$\int_{-a}^{a} k\, \gamma_I d\xi = 2a\, \gamma_o, \qquad (5.52)$$

which is the familiar form of solute balance along an interface at steady state.

6.0 SUMMARY AND RECOMMENDATIONS

In the preceding sections of this report we have addressed the characteristics of solute redistribution in the HgCdTe system from both a theoretical and experimental point of view. Various segments of the work have concentrated on both one-dimensional diffusion and two dimensional aspects of solute redistribution. The overall goal of this effort is to identify and quantify those factors resulting in compositional inhomogeneities in directionally solidified HgCdTe.

The one dimensional model developed in a previous year's work has been applied to several experimental cases and the sensitivity of the model results to variations in thermal gradient and ampoule pull rate examined. Cases in which the ampoule pull rate was changed or in which growth was interrupted for a specific time were modelled to assess the feasibility of using rate changes to identify the interface location and the resulting axial solute profile. Although the utility of the model is limited by its one dimensional nature, it has obvious applicability in selecting certain fundamental processing parameters (ampoule length, pull rate, etc.) to obtain an axial profile with a sufficiently long steady state region.

Although axial solute changes are an unavoidable result of diffusion controlled growth, the presence of radial solute changes may be eliminated under proper growth conditions. The nature and causes of these radial inhomogeneities is to date unknown. We have addressed two main mechanisms for radial solute variations; lateral diffusion due to a curved interface and shape

instability caused by gravity driven flow along a curved interface. These effects are not mutually exclusive, certainly diffusion may take place in the presence of fluid flow. In both cases the interaction of the thermal field and solute distribution in effect determines the interface shape which in turn depends on the driving force for the solute distribution in the liquid. Knowledge of the thermal field and interface shape is fundamental to the application of either a diffusion model or a shape instability model to actual experimental data.

The technique of interface deconvolution provides a method of determining interface shape and composition from analysis of a grown crystal and knowledge of the thermal environment. Several examples of interface deconvolution have been given to illustrate the consequences of an interface with a varying solute distribution being neither an isoconcentrate nor a isotherm. As thermal models are augmented by experimental measurements and improved values of the thermophysical properties, the technique of interface deconvolution will play a large role in determination of the interface shape and composition. These data are vital to the understanding of the causes of compositional variations.

The mechanism of lateral diffusion along a curved interface has been reviewed and comparison to results obtained by other workers has been made for a HgCdTe crystal. Although no definite colclusion can be made at this time, it appears

that the degree of interface curvature necessary to give the experimentally observed radial solute variations is far greater than the curvature that would be expected in normal processing conditions. More refined work in this area is needed.

Finally, we have indicated appropriate equations and boundary conditions for the problem of shape instability. A generalized interface solute balance was derived in the presence of fluid flow. These equations and conservation relations form the basis for perturbation calculations to determine the extent of shape instability. These calculations are to be carried out in the following year.

In order to address all of these issues, certain experimental and theoretical techniques must be applied. Knowledge of the thermal field is paramount to a detailed interpretation of the solute profile. Although we may proceed theoretically using an assumed thermal field and investigate the qualitative behavior of the system, comparison of experiment to theory depends on a detailed knowledge of the actual thermal profile in the crystal. Accordingly, characterization of the growth furnaces should be a first priority. Since it is difficult, if not impossible, to instrument a HgCdTe ampoule, materials of similar thermal conductivity may be used to profile the furnace. At the same time, efforts to obtain the best values for the thermophysical properties of HgCdTe and their temperature

temperature dependence should be undertaken. The furnace profiles can then be used to fine tune the existing thermal models which can then be applied to the HgCdTe growth system. The goal of this effort should be to obtain the best estimate of the thermal profile at steady state.

Analysis of the resulting solute profile in the grown crystal is of obvious importance. Use of the SEM with an energy dispersive spectrometer provides the only method with adequate spacial and compositional resolution. Further work with WDS and improved standards will yield higher absolute accuracy in the x values. Computer assisted analysis of the composition profiles will reduce the time for a complete composition profile. The analysis of the grown crystal coupled with the thermal field can be used to deconvolute the interface shape and composition as described earlier in this proposal.

In order to compare the results of this interface deconvolution with observed values, we must be able to delineate the solid-liquid interface at some point in the growth. Peltier pulsing of the interface is a very renote possibility due to ampoule instrumentation problems. More likely approaches would depend on a rapid quench, decanting, or perturbation of the solute profile by a rate change or shaking of the ampoule. Each of these techniques has distinct advantages and disadvantages. Experiments that compare interface shapes at the same point in growth under the same thermal conditions should be carried out

with the interface marked by a quench, a rate change, and a physical disturbance (vibration, etc.). These interface shapes and compositions may then be compared to those obtained by interface deconvolution.

The effect of ampoule design and early growth conditions must be quantified. Previous experiments have used a conical shaped tip on the ampoule to promote grain selection. Other techniques, such as a neck-down region should be assessed. The extent of thermal coupling plays a large role in determing the initial interface shape. Both experimental and calculation techniques should be used to determine at least the position in the furnace of the first to freeze point.

All of these experiments have been directed towards quantifying the influence of growth parameters (temperature, pull rate, etc.) on the solute profile in the solid. Knowledge of the interface shape and composition is important from a theoretical standpoint if we are to ascertain the role of shape instability.

There are additional experiments that address directly the role of gravity in producing compositional inhomogenities. By a suitable mechanical arrangement, the growth furnace may be tipped at an angle with respect to the g-vector while keeping the ampoule at the center of the thermal field. Crystals grown under these conditions should show a distinct asymmetry in their

solute profile and interface shape if gravity driven fluid flows are important. Convective instabilities not related to those causing shape instability may be present in this case however.

Another experiment represents the extreme limit of the one discussed above. By careful ampoule design, it may be possible to grow in the unstable mode (hot end down) and thus promote thermo-solutal convection rather than suppress it. The value of this experiment should be considered in light of the certain presence of bulk convection which may obscure the effects of shape instability.

Finally, we should seek to discover model systems for HgCdTe. These would be characterized by a material that shows a widely separated liquidus and solidus, rejected component more dense than the bulk liquid, and hopefully transparent to visible light. The essence of shape instability could be best approached experimentally with an ideal model system.

For any set of experiments, the interplay between theory and experiment will follow the general sequence outlined below.

1. Characterize furnace using instrumented ampoule and model material.

2. Apply thermal model to estimate thermal profile to be obtained in HgCdTe ampoule.

3. Use one dimensional model to select growth rate and ampoule length giving the best compromise between length of transient regions, thermal gradients, and ampoule length. We

desire an extended steady state region both compositionally and thermally.

4. Perform experiment

5. Analyze the crystal composition profile using SEM/EDS. Reduce data into appropriate format.

6. Use the interface deconvolution model and the thermal model iteratively to arrive at a self consistent interface shape and thermal field.

7. The fluid flow equations in Section 5 can now be solved using the interface shape, composition and thermal field to give the liquid composition and fluid velocities as a function of g.

If the resulting fluid velocities and liquid composition are consistent with those postulated for causing shape instability, we can conclude that shape instability is a dominant mechanism for creation of radial inhomogeneities and that growth in a microgravity environment should eliminate these inhomogeneities.

In conclusion, we have addressed the key issues and experiments necessary to quantify the causes of solute redistribution in HgCdTe. The results of these experiments and analysis will allow one to identify the extnet of influence of processing parameters on the solute profile. By combining experiment and theory we may then ascertain the degree to which gravity influences this solute redistribution. The ultimate test is then to perform

experiments under microgravity conditions in space.

7.0 REFERENCES

1. M.C. Davidson, Private Communication.

2. S.R. Coriell and R.F. Sekerka, J.Crystal Growth, 46 (1979), 479.

3. S. R. Coriell, R.F. Boisvert, R.J. Rehm and R.F. Sekerka, J. Crystal Growth, 54 (1981), 167.

APPENDIX 1

Copy of the paper

SEGREGATION IN DIRECTIONALLY SOLIDIFIED HgCdTe

Submitted to Journal of Crystal Growth

ONE DIMENSIONAL ANALYSIS OF SEGREGATION IN DIRECTIONALLY SOLIDIFIED HgCdTe

J.C. Clayton[1], M.C. Davidson[2], D.C. Gillies[3], S.L. Lehoczky[4]

ABSTRACT

A one dimensional model for solute redistribution is developed that can be applied to solid solution alloys with widely separated liquidus and solidus phase diagrams. The model is applied to the HgCdTe system and accounts for the variation in interface temperature, segregation coefficient, and growth velocity with composition. The model considers a finite length ampoule, treating both initial and final transient segregation. Agreement between the model and experimental results is good, indicating that the axial solute redistribution in directionally solidified HgCdTe crystals is dominated by diffusion. Comparison of the model to experiment in the final transient region gives values for the effective diffusion constant of $5 \times 10^{-5} cm^2/s$ to $7 \times 10^{-5} cm^2/s$.

1. Semtec, Inc., Huntsville, Alabama
2. Technology Development Corporation, Huntsville, Alabama
3. USRA Visiting Scientist, NASA/MSFC, Huntsville, Alabama
4. McDonnell Douglas Research Laboratories, St. Louis, Mo.

1.0 INTRODUCTION

One of the major problems in production of HgCdTe crystals suitable for large array infrared detectors is material homogeneity. Axial and/or radial composition variations lead to variations in detector response over the area of the detector. Growth techniques that eliminate or minimize these variations are of primary importance in meeting the demands of high quality HgCdTe crystals.

In this work we model the directional solidification growth method with emphasis on the HgCdTe system in an effort to understand those growth parameters influencing crystal uniformity. Our approach is to treat the one-dimensional planar interface solidification problem with no convection, in a similar manner to Favier [1] and other more classical approaches [2,3] with certain important characteristics of the HgCdTe system taken into account.

HgCdTe is representative of a number of alloy semiconductors which form solid solutions over their entire range of compositions. The behavior of the HgCdTe system is such that some of the assumptions made in the studies mentioned above are violated. Figure 1 is a representative pseudo-binary phase diagram for the Hg_{1-x}-Cd_xTe system [4]. Consider an initial liquid with CdTe (solute) mole fraction x=.2. We then find the following characteristics of this system which are different from those found in dilute

alloy systems.

(1) The interface temperature varies from almost 800°C (T_o) initially to 705°C (T_{ss}) at steady state and drops to 668°C over the final transient region of solidification.

(2) The liquidus and solidus curves are widely separated and yield an equilibrium segregation coefficient, k, that varies significantly with liquid composition.

(3) As a consequence of (2), the solid being formed from a liquid in equilibrium with it have widely different compositions. For example, the first-to-freeze solid from a z=.20 mole fraction liquid has x=.54, and steady state results with a x=.055 liquid forming a solid of x=.20.

The goal of this work is to develop a one dimensional model for directional solidification that takes into account the factors above which distinguish the HgCdTe and other solid solution systems from the dilute alloy or doped semiconductor systems treated by previous workers. This model will then be used to analyze the transient segregation experimentally observed in HgCdTe.

2.0 THEORY

In this section we wish to formulate the most general one-dimensional solidification problem in keeping with the directional solidification (Bridgman-Stockbarger) growth configuration and the HgCdTe solid solution system. Accordingly, we will make the following assumptions:

(1) The thermal and concentration fields are one dimensional.

(2) No significant diffusion occurs in the solid.

(3) Convective effects are negligible.

(4) The thermal field is a specified function of the spacial variables and time and does not change as a result of the solidification process.

(5) The sample movement rate, R, is constant. The interface velocity or growth rate, V, is not necessarily constant.

We choose a coordinate system such that z is measured from a fixed laboratory frame (the furnace mid-plane) and x is measured in the sample from the ampoule tip (first-to-freeze point). The variable η is the distance into the liquid

measured from the solid-liquid interface (see figure 2).

Let us denote variables evaluated at the position of the interface by a star (*). Choose t=0 to be the start of solidification in the ampoule tip and $z^*(0)$ the z- co-ordinate of the ampoule tip at t=0. The ampoule is being pulled downward at a rate R with R taken as a positive number. We may then relate the various co-ordinates by

$$x=z+Rt-z^*(0) \tag{1}$$

$$\eta=x-Rt+z^*(0)-z^*(t) \tag{2}$$

The total length of the ampoule is ℓ, and $\ell'=\ell-x^*$ denotes the distance from the interface to the top end (last-to-freeze) portion of the ampoule.

It is most convenient to express the thermal field in the fixed coordinate system, and we shall assume a thermal field of the form

$$T(z,t)=T_o+Gz \tag{3}$$

where G is the thermal gradient, assumed to be constant.

Let L(C) denote the liquidus temperature for material of composition C, and let $C(\eta,t)$ denote the solute (CdTe)

mole fraction in the liquid ahead of the solid-liquid interface. The interface location at any point in time is in effect determined by the thermal field. The solute concentration at the interface is given by C(0,t) and the corresponding liquidus temperature is L(C(0,t)). We may then define the interface location z^* such that

$$T(z^*,t)=L(C(0,t)). \tag{4}$$

The solute concentration in the liquid satisfies

$$D\,\frac{\partial^2 C}{\partial \eta^2} + V(t)\,\frac{\partial C}{\partial \eta} = \frac{\partial C}{\partial t}\,, \tag{5}$$

where D is the effective diffusion constant and V(t) is the growth velocity. The boundary conditions are

$$C(\eta,0) = C_o \qquad\qquad t=0 \tag{6}$$

$$\frac{\partial C(\eta,t)}{\partial \eta} = 0 \text{ at } \eta=\ell' \text{ for all } t \tag{7}$$

$$V(t)\,(k(C) - 1)\,C(0,t) = D\,\frac{\partial C(0,t)}{\partial \eta} \qquad t>0. \tag{8}$$

The boundary condition in eq. (7) is normally written for an infinite ampoule as, $C(\eta,t) = C_o$ as $\eta \to \infty$ for all t. In this study we wish to solve for both the initial and final solidification transients, hence we require that there be no source of solute at the ampoule end ($\eta = \ell'$) giving the boundary conditions in eq. (7).

In addition to the above equations, we shall assume that the liquidus portion of the phase diagram over the region of interest may be approximated by

$$L(C) = T_A + M_A C + \gamma C^2 \tag{9}$$

where T_A, M_A and γ are appropriate constants obtained by least-squares fitting. We may then write

$$V(t) = R + \frac{dz^*}{dt} \tag{10}$$

where z^* satisfies

$$T(z^*,t) = L(C(0,t)). \tag{11}$$

Using the assumed expressions for the thermal field and the liquidus curve we find

$$z^*(t) = 1/G(T_A - T_o + M_A C(0,t) + \gamma C^2(0,t)), \qquad (12)$$

giving

$$\frac{dz^*}{dt} = (1/G)(M_A + 2\gamma C(0,t)) \frac{\partial C(0,t)}{\partial t} \qquad (13)$$

The numerical procedure used to solve equations (5) to (8) is unique. Let the incremental time and spacial steps be Δt and $\Delta\eta$ respectively. Assume at time t_o the values of $C(\eta,t)$ have been determined for all $t \leq t_o$ and all η. The goal is to then compute $C(\eta,t')$ for all η where $t' = t_o + \Delta t$. We assume a trial value C^* for the concentration at the interface at time t', say

$$C(0,t') = C^*. \qquad (14)$$

We then compute

$$\frac{\partial C(0,t')}{\partial t} = \frac{C^* - C(0,t_o)}{\Delta t} \qquad (15)$$

giving the interface velocity

$$V(t')=R+\frac{dz^*}{dt}\Big|_{t=t'} =R+(1/G)(M_A+2\gamma C^*)\ \frac{\partial C(0,t')}{\partial t} \quad . \quad (16)$$

We may then compute the first spacial derivative via the boundary condition (eq. 8) as

$$\frac{\partial C(0,t')}{\partial \eta} = (1/D)V(t')(k(C^*) -1)\ C(0,t') \qquad (17)$$

where $k(C^*)$ is determined by the phase diagram and is in practice obtained by interpolation in a table of values for k versus C. The second derivative is found via the diffusion equation (5) giving

$$\frac{\partial^2 C(0,t')}{\partial \eta^2} = (1/D)\ \left(\frac{\partial C(0,t')}{\partial t} - V(t')\ \frac{\partial C(0,t')}{\partial \eta}\right) \quad (18)$$

We then may obtain our desired results by expansion

$$C(\Delta\eta,t')=C(0,t')+\frac{\partial C(0,t')}{\partial t}\ \Delta\eta\ +\frac{\partial^2 C(0,t')}{\partial t^2}\qquad \frac{\Delta\eta^2}{2} \quad (19)$$

for the value of the concentration in the liquid a distance $\Delta\eta$ away from the interface.

We now propogate $C(\eta,t)$ out in until the end of the ampoule is reached ($\eta=\ell'$) and test to see if the boundary condition

$$\frac{\partial C}{\partial \eta}\ (\eta,t')=0 \text{ at } \eta=\ell' \tag{20}$$

is met. The solution may be propagated to $\eta' = 2\Delta\eta$, the next spacial step, by first calculating

$$\frac{\partial C(\Delta\eta,t')}{\partial t} = \frac{C(\Delta\eta,t')-C(\Delta\eta,t_o)}{\Delta t} . \tag{21}$$

We then use a Taylor series expansion and the diffusion equation to obtain

$$\frac{\partial C(\Delta\eta,t')}{\partial \eta} = \frac{\partial C(0,t')}{\partial \eta} + \frac{\partial^2 C(0,t')}{\partial \eta^2}\ \Delta\eta \ , \tag{22}$$

and

$$\frac{\partial^2 C(\Delta\eta,t')}{\partial \eta^2} = (1/D)\left(\frac{\partial C(\Delta\eta,t')}{\partial t} -V(t')\frac{\partial C(\Delta\eta,t')}{\partial \eta}\right). \tag{23}$$

A second expansion leads to the desired results

$$C(2\Delta\eta,t')=C(\Delta\eta,t')+\frac{\partial C(\Delta\eta,t')}{\partial\eta}+\frac{\partial^2 C(\Delta\eta,t')}{\partial\eta^2}\frac{\Delta\eta^2}{2} \quad . \quad (24)$$

The same process is used for the next spacial step $3\Delta\eta$, etc. until $\eta=\ell'$, the end of the ampoule at this time step. A test is made to see if the boundary condition eq. (20) is satisfied. If it is not, a new trial value of C^* is selected and the entire process repeated until the boundary condition is satisfied.

The initial value boundary condition

$$C(\eta,0)=C_o \quad (25)$$

allows one to take $t_o=0$ and proceed in a straightforward manner to calculate $C(\eta,t)$ for any t. At each time step, after the value of $C(0,t)=C^*$ has been found that satisfies the boundary condition in eq. (20), we may find the solute concentration in the solid as

$$C_s(x^*) = k(C(0,t))\ C(0,t) \quad (26)$$

where we note that $z^*(t)$, and thus $x^*(t)$, are determined by the thermal field and liquidus curve of the phase diagram. The remaining amount of liquid is given by

$$\ell' = \ell - x^* \tag{27}$$

The time is incremented by Δt, and the entire process repeated to yield new values of $x^*(t)$, $z^*(t)$, $V(t)$, and $C_s(x^*)$.

3.0 RESULTS

In this section we present results from the model and compare these results to experimental solute profiles obtained from directionally solidified HgCdTe crystals. In figure 3 we present a typical solid concentration as a function of position taken for an initial liquid composition of x=.2. Theoretical curves of solid composition are plotted for two different values of the diffusion coefficient $D=5x10^{-5}cm^2/sec$ and $D=7x10^{-5}cm^2/sec$. We note the initial transient region marked by a decreasing solute concentration, a steady state region extending some 105mm, and a final transient in which the solute concentration tends to zero as the end of the ampoule is reached. A solute distribution of this nature is typical for a segregation coefficient $k>1$, and in fact k varies from 2.7 initially to 3.6 in the steady state region. At this translation rate, the transient regions are rather short, and the differences between the curves with different diffusion constants are most marked in the final transient region.

In figure 4 we plot both the growth velocity and interface position relative to the furnace as a function of distance along the crystal. The other input data is the same as in figure 3 and we chose $D=5x10^{-5}cm^2/sec$. The thermal field is assumed to be such that the steady state solidification temperature (705°C) occurs at the furnace midplane (z=0). As

a consequence of the phase diagram, the first to freeze from a x=.20 liquid occurs at a higher temperature (∿800°C) and consequently is located higher in the furnace. As solute is preferentially incorporated, a diffusion layer is established and the liquid composition in front of the interface approaches the steady state value of x=.055 which solidifies at a temperature of 705°C. During the approach to steady state, the interface position changes, moving toward the furnace midplane. Thus the interface moves along with the ampoule toward the cooler portion of the furnace, although not at the ampoule pull rate R. At steady state, we have a fixed solidification temperature and hence a fixed interface position in the furnace. As the end of the ampoule is approached, there is no longer enough solute remaining in the liquid to replenish the diffusion layer, resulting in a decreased solute composition at the interface. This, in turn, results in a still lower solidification temperature and consequently the interface position moves toward the cold end of the furnace.

The growth velocity, or the velocity of the interface relative to the ampoule tip is also shown on figure 4. As discussed above, the interface moves down toward the furnace midplane during the initial transient region, resulting in a growth velocity that is initially zero and increases until the steady state region is reached. At steady state the interface is fixed with regard to the furnace and consequently the growth

rate and ampoule pull rate are equal. The final transient region presents some rather unexpected behavior. As the solute is exhausted in the remaining liquid during the final transient, the solidification temperature decreases and the interface again moves along with the ampoule toward the cold zone, resulting initially in a growth rate less than the translation rate. At the very end of the ampoule, both the solute concentration and the concentration gradient in the liquid approach zero due to the boundary condition at the ampoule end. As a consequence, the time rate of change of solute concentration at the interface also approaches zero, resulting in the velocity increasing back to the ampoule pull rate at the ampoule end. The numerical scheme used here may over-estimate the length of this region due to a finite node size, but the effect is present, though of little technological importance.

We have indicated some features of the model as it applies to the HgCdTe system. Figure 5 shows a plot of experimentally measured solute concentrations and calculated solute profiles from the model. The data is taken from a HgCdTe crystal with C_o=.20 and an estimated thermal gradient of 200°C/cm. In this instance the translation rate was .762mm/hr. The experimental data points were determined by using an SEM with an energy dispersive spectrometer and HgCdTe standards to permit peak deconvolution [5]. Since radial concentration variations occur in

this system, the axial composition profile is an area-weighted average of the radial compositions across each slice at a particular axial position. The results of such a procedure would be equivalent to those obtained by density measurements.

There are several features to note in figure 5. Agreement between the model and data in the initial transient region is not very good. This may be due to several effects. Initial solidification occurs in a conical ampoule tip, conditions which do not approximate those assumed here. Secondly, although not shown on this graph, the experimental data shows an initial increase in solute concentration in the tip of the crystal before it begins to decrease. This is thought to be due to undercooling which certainly must occur to some extent and can lead to nucleation away from the tip. The net result of this is to cause the initial transient region to occur further along the crystal then anticipated. resulting in disagreement with the calculated curves.

In the steady state region, agreement between experiment and theory is quite good as would be expected. The data lies below the calculated curve as the final transient region is approached. Although the experimental analysis has a resolution od $\Delta z \sim \pm$ .002, the availability of absolute standards my limit the absolute accuracy of these measurements. In addition, in the model computational time constraints result in chosing a spacial and time step size sufficiently coarse as to yield accumulated truncation errors in the later stages, giving a steady state value of x=.205 instead of x=.200. Taking both of these effects

into consideration, the agreement is good for a model with no feedback from the experimental data.

The final transient region is best examined on an expanded scale. Figure 6 is an enlarged portion of the final transient region. In this case the experimental data have been shifted upward and the calculated curve downward to yield a value of $x=.2$ in the steady state. In addition, the calculated curve has been shifted toward the origin very slightly to account for errors in position measurement. The same corrections were applied to all data points shown, hence we are in a sense adjusting the data to conform to the calculated curve but have not changed the shape of the data curve. It is apparent that the shape of the data curve most closely fits a value of the effective diffusion constant $D=7\times10^{-5}cm^2/sec$. We note that the shape of the calculated curve for $D=5\times10^{-5}cm^2/sec$ is not consistent with the data even if we translate the position of the data points. In other crystals grown under different thermal fields and translation rates, we have found that the experimental final transient curve is always fit using values for D between $5\times10^{-5}cm^2/sec$ and $7\times10^{-5}cm^2/sec$ [6].

4. CONCLUSIONS

We have presented a one dimensional model for calculation of axial solute distribution in the HgCdTe solid solution system.

The model accounts for the change in interface temperature, segregation coefficient, and growth velocity due to a widely separated liquidus and solidus phase diagram. The model also accounts for the effects of a finite length ampoule, allowing the final transient segregation to be calculated.

As a consequence of the phase diagram, we see that the interface velocity and position vary over the initial transient, remain constant in the steady state, and vary again over the final transient. The implications of this are that obtaining flat solidification isotherms over the entire region of growth in a real furnace system can be difficult if we must also maintain a high thermal gradient.

By comparing experimental results to calculated curves in the final transient region, we conclude that the effective diffusion constant in the HgCdTe system lies between $5 \times 10^{-5} cm^2/sec$ and $7 \times 10^{-5} cm^2/sec$ for an initial liquid composition of $C_o = .20$.

Agreement between experiment and theory is good indicating that diffusion dominates the axial segregation in the HgCdTe system. In a subsequent paper, we will treat the two dimensional problem and interface stability.

ACKNOWLEDGEMENTS

This work was funded under NASA contract NAS8-33698 (Clayton) NAS8-33107 (Lehoczky) and NAS8-33445 (Gillies) as part of the Materials Processing in Space program. The authors wish to ack-

nowledge the support of F.R. Szofran, A. Dorries, and L. Holland for their work in growth and characterization of HgCdTe samples.

REFERENCES

[1] J.J. Favier, J. Crystal Growth 49 (1980) 373.

[2] W.A. Tiller and K.A. Jackson, Acta Met.1 (1953) 428.

[3] V.G. Smith, W.A. Tiller and J.W. Rutter, Can. J. Phys. 33 (1955) 723.

[4] F.R. Szofran and S.L. Lehoczky, J. Electronic Material 10 #6 (1981) 1131.

[5] D.C. Gillies, submitted for publication in J. Electronic Materials.

[6] S.L. Lehoczky and F.R. Szofran, Private Communication.

FIGURE CAPTIONS

FIGURE 1 - Pseudo-binary phase diagram of $Hg_{1-x}Cd_xTe$.

FIGURE 2 - Co-ordinate system used in model. The ampoule tip is at z^* (o) at t=o.

FIGURE 3 - Calculated solid axial solute concentration versus distance along the crystal. Curves for $D=5x10^{-5}cm^2/s$ and $7x10^{-5}cm^2/s$ are shown.

FIGURE 4 - Interface velocity and location relative to the furnace as a function of distance along the crystal. The scale is broken to eliminate the constant steady state region. Input parameters to the model are the same as in figure 3.

FIGURE 5 - Comparison of experiment and model results for a directionally solidified crystal. The initial liquid composition was z=.20. Calculated curves are shown for $D=5x10^{-5}cm^2/s$ and $D=7x10^{-5}cm^2/s$.

FIGURE 6 - Enlargement of the final transient region of figure 5. The data and calculated curve have been shifted to yield the best agreement (see text). The upper curve is calculated with $D=5x10^{-5}cm^2/s$ and the lower curve with $D=7x10^{-5}cm^2/s$.

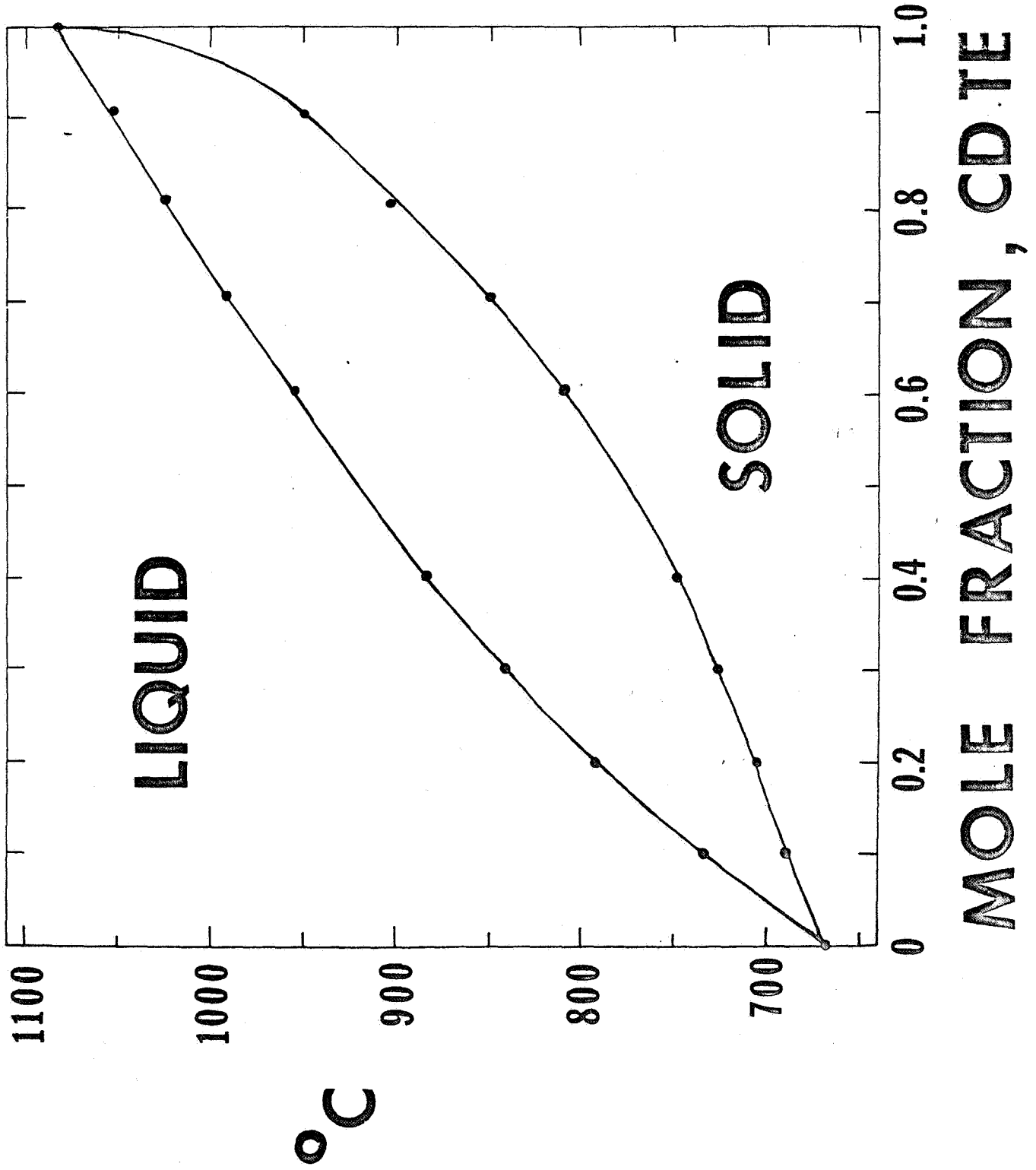
LIQUID
SOLID
°C
1100
1000
900
800
700
0
0.2
0.4
0.6
0.8
1.0
MOLE FRACTION, CDTE

FIGURE 1

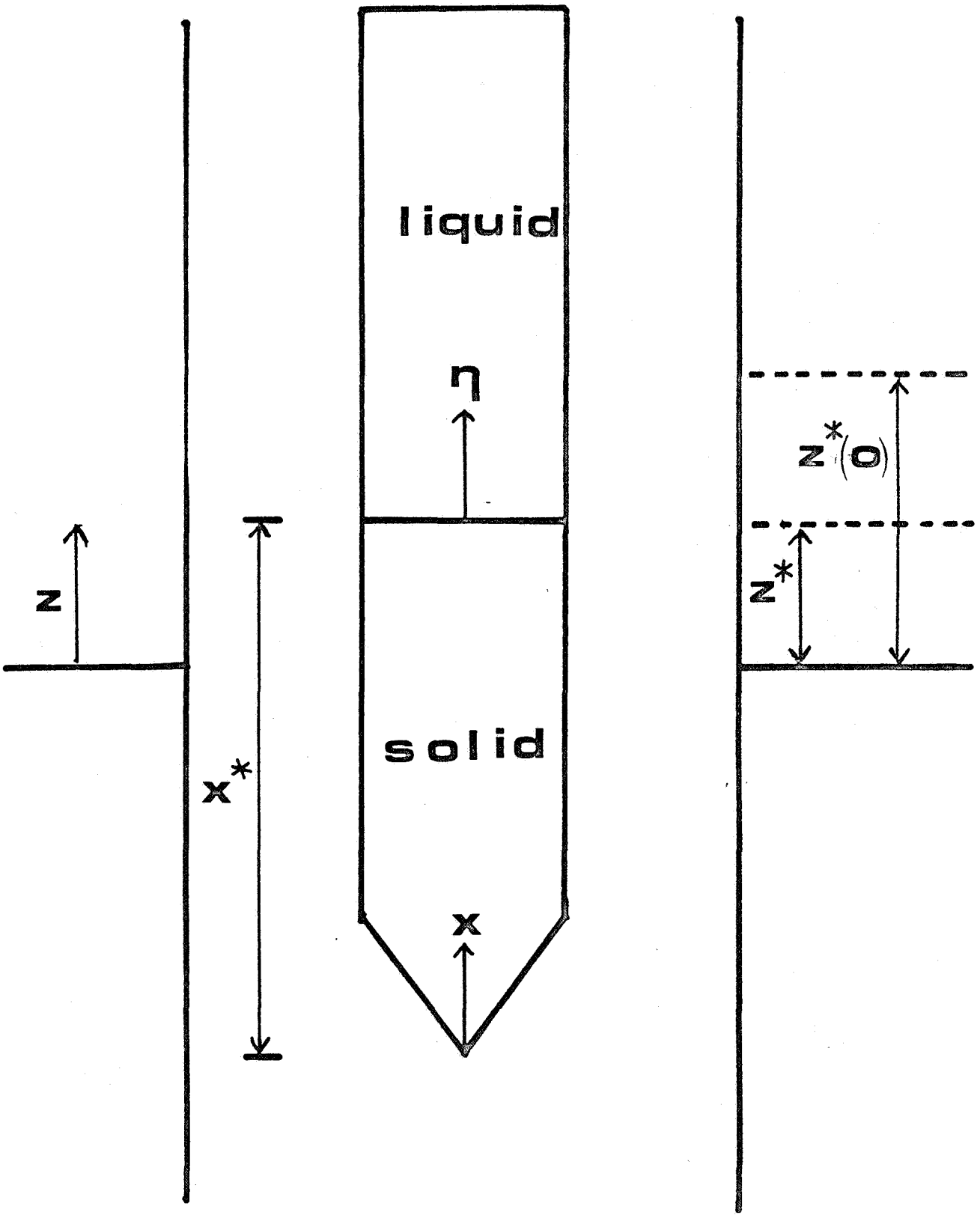

FIGURE 2

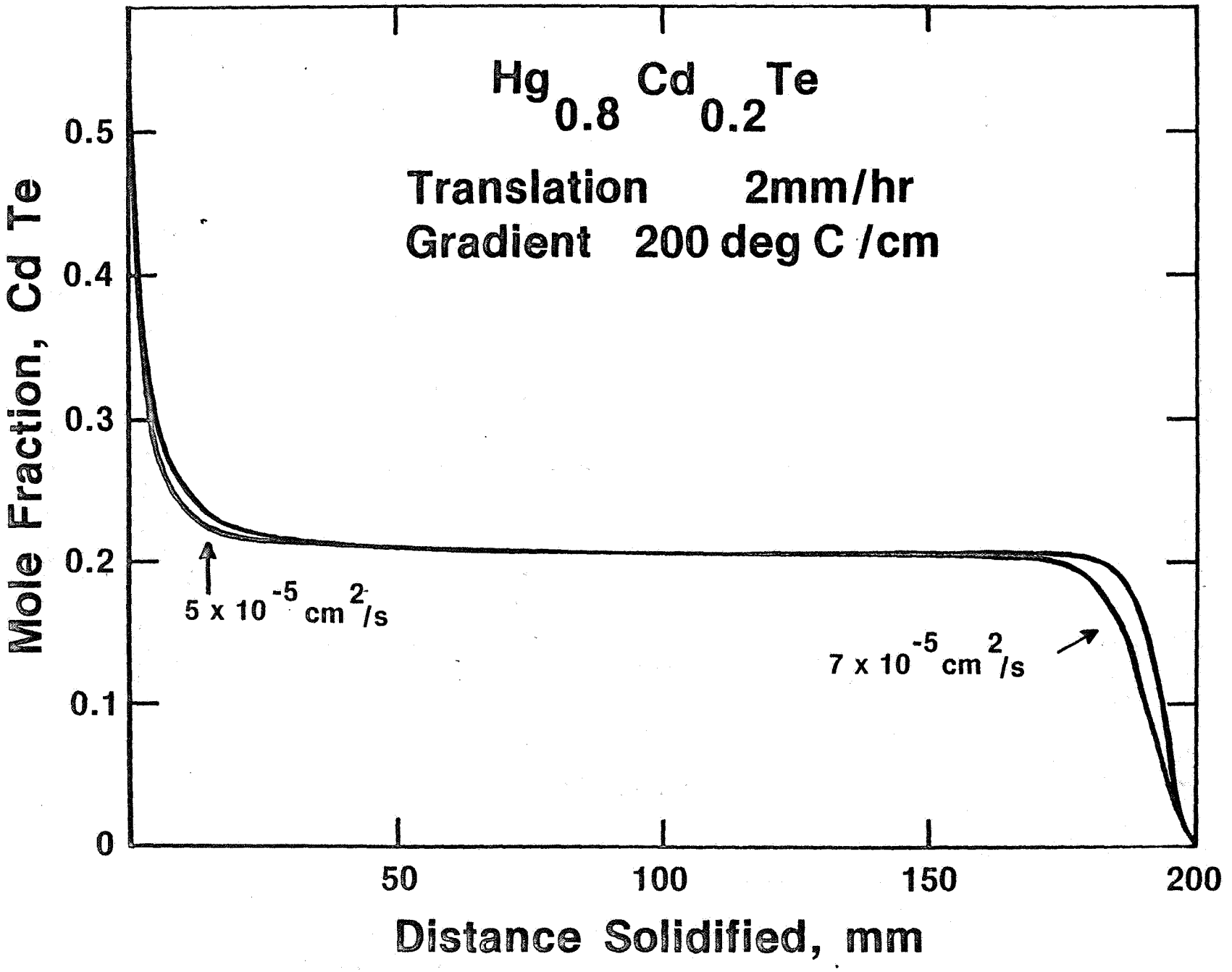
Hg 0.8 Cd 0.2 Te
Translation 2mm/hr
Gradient 200 deg C /cm
Mole Fraction, Cd Te
0.5
0.4
0.3
0.2
0.1
0
5 x 10 -5 cm 2/s
7 x 10 -5 cm 2/s
50
100
150
200
Distance Solidified, mm

FIGURE 3

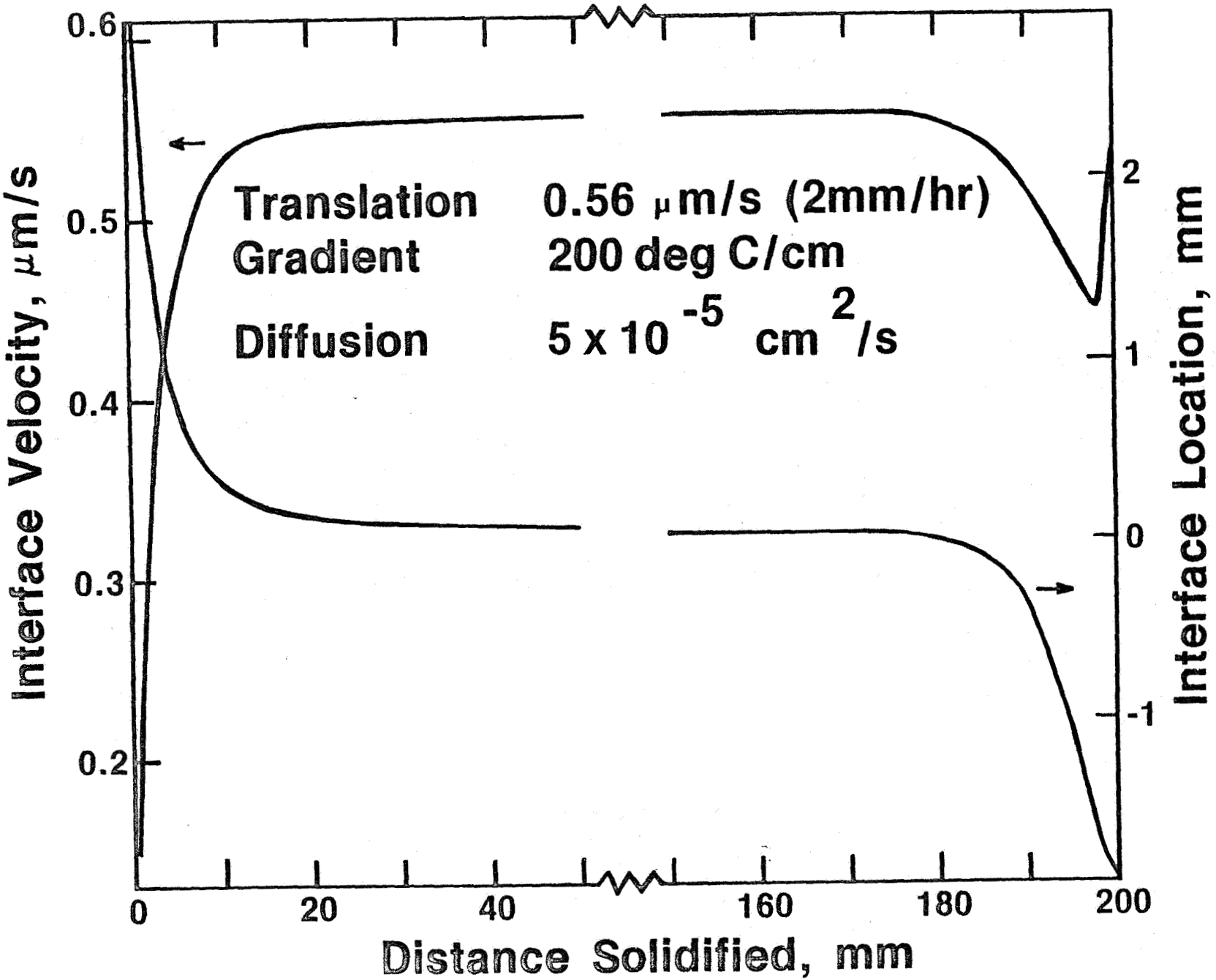
Translation 0.56 μm/s (2mm/hr)
Gradient 200 deg C/cm
Diffusion 5 x 10 -5 cm 2 /s
Interface Velocity, μm/s
Interface Location, mm
Distance Solidified, mm
0.6
0.5
0.4
0.3
0.2
2
1
0
-1
0
20
40
160
180
200

FIGURE 4

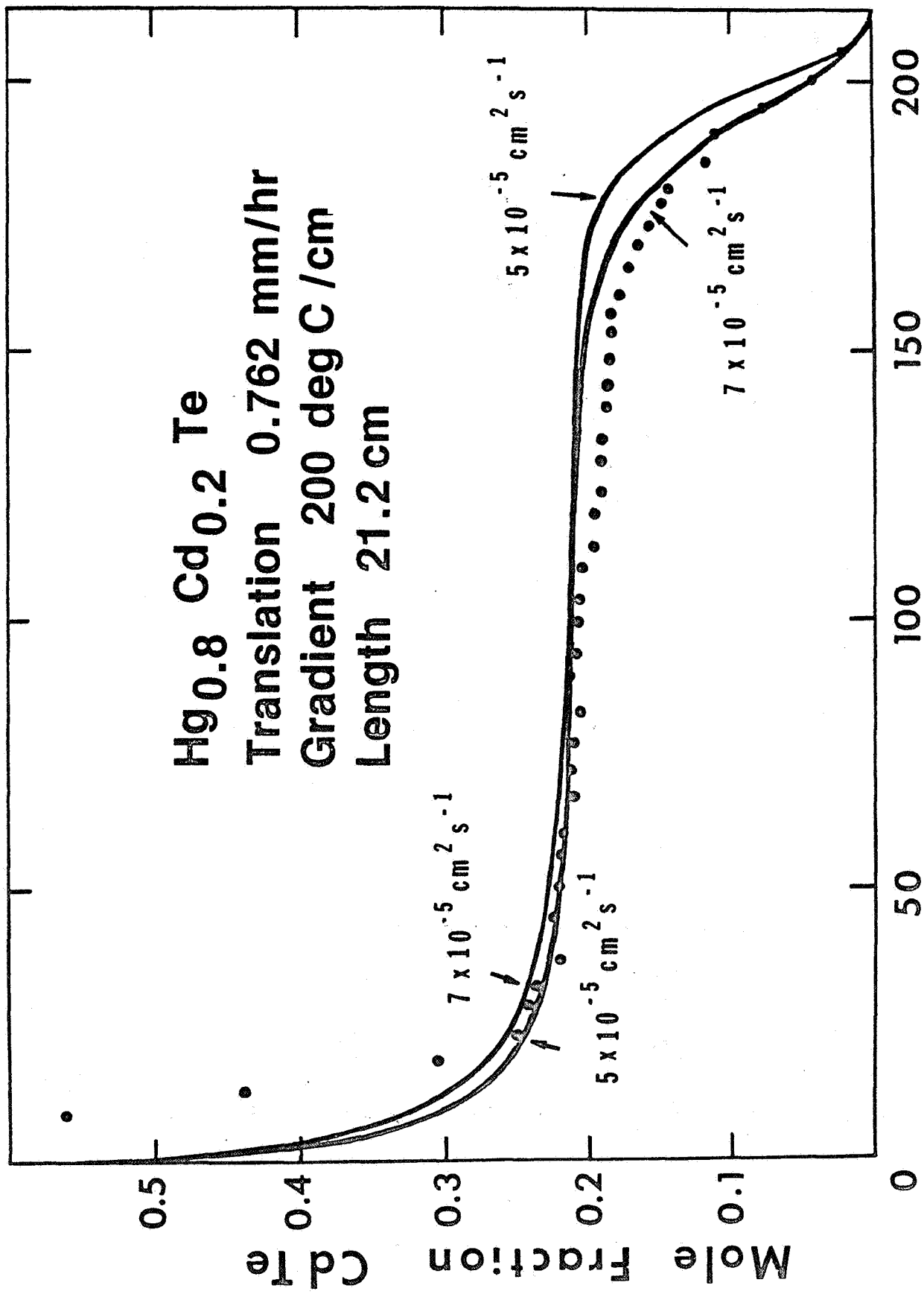
Hg0.8 Cd0.2 Te
Translation 0.762 mm/hr
Gradient 200 deg C/cm
Length 21.2 cm
7 x 10-5 cm2 s-1
5 x 10-5 cm2 s-1
5 x 10-5 cm2 s-1
7 x 10-5 cm2 s-1
Mole Fraction CdTe
0.5
0.4
0.3
0.2
0.1
0
50
100
150
200
Distance Solidified mm

FIGURE 5

Mole Fraction, CdTe
0
0.1
0.2
120
160
200
Distance Solidified, mm

FIGURE 6

APPENDIX 2

Preliminary copy of the paper

INDIRECT DETERMINATION OF THE INTERFACE IN SOLID SOLUTION CRYSTALS

To be submitted to Journal of Crystal Growth

INDIRECT DETERMINATION OF THE INTERFACE IN SOLID SOLUTION CRYSTALS

Donald C. Gillies and James Creed Clayton
Semtec Incorporated, Huntsville, Alabama 35805

ABSTRACT

A technique is described by which the location, shape and solid composition of the solid-liquid interface in a solid-solution crystal is determined by indirect means. The method utilizes experimentally measured composition data from the solidified crystal together with thermal profiles calculated from a thermal model to iteratively determine interface parameters consistent with both thermal boundary conditions and the measured solute distribution. This technique allows for an interface that may be neither an isoconcentrate nor an isotherm. Typical interface shapes in HgCdTe crystals derived by this technique are given as examples.

1.0 INTRODUCTION

Solid solutions are presently being utilized in several semiconductor applications with promise for wider applicability in the future. Mercury cadmium telluride (HgCdTe), for example, shows superior performance as a radiation detector in the short to medium infrared region with potential for extension to longer wavelengths. The directional solidification of solid solutions has, however, met with limited success. Apart from the chemical and structural problems of a particular system, directionally solidified solid solutions show pronounced compositional inhomogeneities. These inhomogeneities limit the materials yield for single devices and the performance of large area arrays. These compositional inhomogeneities, present to some degree in most solid solutions, depend to a large degree on the shape of the solidifying interface. The determination by experimental and theoretical means of the interface shape during the undirectal solidification of a solid solution system is the subject of this paper.

In the HgCdTe system the high degree of preferential incorporation of CdTe leads to severe inhomogeneities. Proper choice of ampoule length and crystal pull rate will result in a steady state growth region with a constant axial solute composition, however, compositional analysis of crystals indicate that there still exists a high degree of radial segregation.

The cause of this radial segregation is largely unknown. Possible mechanisms include lateral diffusion across a curved interface (1,2) convective effects and thermal effects (3,4). Another postulated mechanism in HgCdTe is a result of the heavier rejected component (HgTe) flowing along a curved interface leading to higher concentrations of HgTe at the lowest points in the interface. If the interface were concave, the increased HgTe concentration at the center of the interface would lead to a lowering of the solidus temperature at the center relative to the edges, further increasing the curvature of the interface. This global interface instability has been termed shape instability by Davidson (5) and has been observed in other systems in which the rejected component is more dense than the bulk liquid (6).

In any of the above mechanisms for radial compositional variations, the shape and composition of the solid-liquid interface is an important factor. Knowledge of the shape of the interface at various points in the crystal during growth is required in order to determine the causes of radial compositional variations and to design growth procedures that minimize these variations. The high mercury vapor pressure in HgCdTe makes instrumentation of the ampoule very difficult; thus traditional means of interface demarcation by Peltier pulsing cannot be used. The purpose of this paper is to indicate a method by which the interface shape and com-

position may be inferred from estimates of the thermal field and measured composition data taken from the grown crystal. The consequences of interface curvature in a system with a highly sloping liquidus and solidus curve such as HgCdTe upon compositional variations is indicated and experimental examples are presented.

2.0 INTERFACE DECONVOLUTION - THEORY

We wish to formulate the general problem of an alloy being directionally solidified at a constant pull rate R. Choose a co-ordinate system x,y,z fixed to the sample with the y-axis aligned with the sample axis and anti-paralled with the gravity vector $\bar{g}$ (positive y is up, toward the liquid). The following equations relate the fluid velocity $\bar{u}$ and concentration C.

$$\bar{\nabla}\cdot\bar{u} = 0, \tag{1}$$

$$\frac{\partial u}{\partial t} + (\bar{u}\cdot\bar{\nabla})\bar{u} = -1/\rho_o\ \bar{\nabla}P+\nu\nabla^2\bar{u}+\bar{g}\ (\rho/\rho_o-1), \tag{2}$$

$$\frac{\partial C}{\partial t} + \bar{u}\cdot\bar{\nabla}C = D\nabla^2C, \tag{3}$$

where P is a pressure, ν the kinematic viscosity, ρ the fluid density, D the liquid diffusion constant and t is time. We have assumed that diffusion in the solid is negligible and that the material properties are independent of concentration and temperature except for the difference between liquid and

solid. The above equations represent the simplified Oberbeck-Boussinesq approximation.

The thermal field is best written initially in a furnace fixed frame $\hat{x},\hat{y},\hat{z}$ whose origin is at the furnace midplane. If V is the media velocity seen from the furnace frame, we have

$$\frac{\partial \hat{T}}{\partial t} + \bar{V}\cdot\bar{\nabla}\ \hat{T} = \kappa\nabla^2\hat{T}, \tag{4}$$

with κ the thermal diffusivity and T the temperature. Boundary conditions for eqn. (4) must specify an initial value for the thermal field $\hat{T}(\hat{x},\hat{y},\hat{z},0)$, and either a temperature over some surface or the thermal flux across that surface. The thermal problem and its means of solution is well known, however problems in solidification are complicated by the presence of the solid-liquid interface in the sample. At the interface we have an additional boundary condition

$$k_L\ (\bar{\nabla}\hat{T}\cdot\hat{n})_L = k_s(\bar{\nabla}\hat{T}\cdot\hat{n})_s\ , \tag{5}$$

with $\hat{n}$ the normal to the interface, k_L and k_s the thermal conductivity of the liquid and solid, respectively. Here we have assumed that the solidification velocity is sufficiently slow that latent heat effects are ignorable. The thermal field equations may be transformed to the sample fixed co-ordinate system with $x=\hat{x}$, $y=\hat{y}+Rt-y_o$, $z=\hat{z}$, where y_o is the position of the sample

tip at t=0. We relate the media velocity V to the pull rate and fluid velocity u by

$$\bar{V} = \bar{R} + \bar{u} \tag{6}$$

where $\bar{R}$ =(0,-R,0) and $\bar{u}$=0 in the solid. The boundary conditions specifying the thermal field must be transformed into the sample-fixed coordinate system and in general will be a function of time. The resulting equation for the thermal field in the sample fixed co-ordinate system becomes

$$\frac{\partial T}{\partial t} + \bar{u}\cdot\nabla T = \kappa \nabla^2 T \quad , \tag{7}$$

and the boundary conditions must be transformed into the sample co-ordinate system.

The boundary conditions for eqns.(1-3)may be written in the sample co-ordinate system as

$$C(y\to\infty) = C_o \tag{8}$$

$$\bar{v}\cdot\hat{n}\ (C_{sI}-C_I) = \rho_L/\rho_s\ D\ \ \bar{\nabla}C\cdot\hat{n} \quad \text{at the interface,} \tag{9}$$

$$C_{sI} = k\ C_I \qquad \text{at the interface,} \tag{10}$$

$$\bar{v} \cdot \hat{n} \, (\rho_L - \rho_s) = (\bar{u} \cdot \hat{n}) \, \rho_L \quad \text{at the interface,} \tag{11}$$

$$T_I = f(C_I) \tag{12}$$

$$\rho = \rho(c,T) \quad . \tag{13}$$

Equation (8) assumes an infinite sample with the bulk liquid solute concentration C_o. Equation (9) is the solute conservation relation applied at the interface where $\bar{v}$ is the solidification velocity, C_I denotes the solute concentration in the liquid at the interface, C_{sI} the solid solute concentration at the interface and the solid and liquid densities ρ_s and ρ_L are also evaluated at the interface, Equation (10) relates C_{sI} to C_I via the equilibrium segregation coefficient k. Equation (11) is a condition on the normal component of the fluid velocity at the interface, and we also assume the tangential component of $\bar{u}$ vanishes at the interface (no-slip condition). The temperature at the interface is determined via the phase diagram, and equation (12) relates the liquid interfacial composition C_I to the liquidus temperature via the function f, i.e. f is the liquidus curve of the phase diagram. Equation (13) expresses the density as some proscribed function of the concentration and temperature. We have assumed there is no undercooling and that capillarity effects are ignorable.

The set of equation (1-4) together with their boundary conditions represent the general description of an alloy undergoing directional solidification. Several authors (1,2) have addressed the solution

to these equations using perturbution techniques. In a later paper, we will approach the problem of shape instability utilizing these equations. For the purposes of this paper, we wish to describe a different approach that allows, under certain circumstances, the problem described above to be solved for the interface shape and concentration, without solving explicitly the rather formidable set of equations.

We begin by assuming that we have analyzed a crystal grown by directional solidification and determined the solid solute concentration profile. For the sake of description, we will assume that the crystal is azimuthally symmetric so that we have a two dimensional problem. Let $C_s(x,y)$ be the solid composition profile measured on the crystal. In actual practice, we measure the solid solute concentration at discrete points; a polynomial fit may then be used to construct $C_s(x,y)$.

Futhermore, we assume that the furnace is sufficiently well characterized that a thermal model based on equation (4) will yield a thermal field sufficiently accurate for our purposes. At some point in time, we assume as an initial guess the position and shape of the solid-liquid interface. A thermal model together with appropriate boundary conditions is used to calculate a trial thermal field $T(x,y)$, utilizing the assumed interface shape and position to apply the thermal boundary condition at the interface.

We also use the solidus curve of the phase diagram $S(C_s(x,y))$,

where S is the solidus temperature for the solute composition $C_s(x,y)$ and we assume no undercooling is present. We thus have two temperature distributions at any point in time in the crystal; the temperature at which each point froze $S(C_s(x,y))$, and the calculated temperature in the crystal at each point, $T(x,y)$.

The solid-liquid interface is the locus of all points whose solidification temperature $S(C_s(x,y))$ is equal to the temperature $T(x,y)$ at that point in time. We have implicitly assumed that both S and T are monotonic functions, i.e. growth conditions are such that there is only one interface and the liquid is never constitutionally supercooled.

We may form a function $I=S(C_s(x,y))-T(x,y)$ which gives the interface location x^*,y^* by setting

$$I(x^*,y^*) = 0, \tag{14}$$

that is, the zeros of $I(x,y)$ are the interface co-ordinates at that point in time.

The interface position calculated by this "deconvolution" procedure may not be the same as assumed initially to calculate the thermal field $T(x,y)$. We now use the new interface co-ordinates in the thermal model to calculate a new thermal field. We should note that we now have an interface position and the temperatures along that interface; this is a boundary condition in calculating

the new thermal field. The new thermal field is used with the measured concentration data (which does not change) in the deconvolution procedure described above to calculate new interface co-ordinates x^*, y^*. This iteration procedure continues until we find interface co-ordinates that do not change from the previous iterations. The final result is an interface location together with a self-consistent thermal field that are both consistent with the measured solid solute profile. The flow chart in Figure 1 indicates the steps involved in the iteration procedure.

In essence, this procedure substitutes experimentally measured concentration data for solving the coupled solute equations. The thermal model must assume that heat transport due to fluid motion is ignorable. The iteration procedure retains the coupling of the solute equation and the thermal field which involves equations (3,4,9,and 12). Upon convergence, we have interface co-ordinates that are self-consistent with the boundary conditions for the thermal field and the experimentally measured solute profiles. We have not, however, determined the solute profile in the liquid ahead of the interface and thus have not solved for $\bar{u}$ in equations (1 and 2).

Convergence limits of this iterative procedure have not yet been established. It is in the nature of a compact transformation, so that convergence will be assured within a region sufficiently close to the final valve. To date, this iterative procedure has not been carried out and thus the constraints on the initial guess for the interface location to insure convergence have not been determined. Examples of the deconvolution process and how various

thermal fields affect the interface shape in HgCdTe are given in the following section.

3.0 INTERFACE DECONVOLTION - EXAMPLE

Although a complete treatment of the solidification problem would require carrying out the iteration process described above, we may illustrate the deconvolution method by a simple example. Figure 2 is a plot of measured isoconcentration lines converted into solidification temperatures using the pseudo-binary phase diagram for HgCdTe for a crystal grown under directional solidification. The solute concentration values were measured at discrete points along the crystal using an SEM with an energy dispersive spectrometer. This discrete data was then fit to a polynomial at each radial (x-value) point and interpolated to obtain isoconcentration lines. The concentration was converted via the phase diagram to an equivalent solidus temperature which is indicated on the diagram. These data are far from ideal, but do indicate the magnitude of radial segregation present in directionally solidified HgCdTe crystals. The abrupt drop in the isoconcentration lines at the right hand edge of the crystal cannot be explained in terms of the simple model presented here, we have ignored these data points in our analysis.

The central issue is that if we assume that the solid-liquid interface is of uniform composition and hence an isotherm we must

interpret the composition data in Figure 2 as indicating a extremely curved interface shape and consequently highly curved isotherms. However, there is no reason to assume that the interface is of uniform composition. Convection, lateral diffusion, and shape instability all may act to create an interface that is neither an isotherm nor an isoconcentrate. We may illustrate the magnitude of this effect by computing an interface shape consistent with the data in Figure 2 for various trial thermal fields.

Figure 3 is a schematic of two typical thermal profiles that might be obtained in a crystal growth experiment. These thermal fields are not specific to any furnace or sample configuration but are used as examples only. They are, however, representative of the types of isother disstributions obtained in HgCdTe from thermal models.

The interface location is deconvoluted from the data contained in Figures 2 and 3. At selected radial (x-value) positions the axial composition data is converted via the phase diagram to a solidus temperature and fit to a least squares polynomial giving a function $S_x(C(y))$ for each selected x-value. In a similar manner the thermal data is fit to a polynomial yielding $T_x(y)$. We note that in general the thermal field expressed in the sample is a function of time and sample pull rate. In this example we assume that the thermal field has attained its steady state value and that growth velocities are sufficiently slow that heat transfer due to sample motion does not perturb the thermal field.

Given $S_x(C_s(y))$ and $T_x(y)$ we find the zero of $I_x(y) = S_x(C_s(y)) - T_x(y)$ for each x value which gives the interface co-ordinates x^*, y^*. The results are illustrated in Figure 4. For each assumed thermal field two different interface positions are shown; the number at the right hand side is the approximate location of the interface in mm along the solidified sample. The mid-plane is the location of the flat isotherm in each thermal profile. The two interfaces do not exist at the same point in time of course, but rather are calculated at different times in the growth. The time interval between the interface at 32mm and the interface at 101mm is 90 hours. The sample translation rate was 0.762 mm/hr.

Figure 4 indicates that despite the highly curved isoconcentration lines shown in Figure 2, we find that only a slight curvature in the interface results from the typical thermal fields assumed here. The implications are that very small interface curvatures lead to gross radial segregation in HgCdTe. The first thermal field yields interfaces in a region of convex isotherms while the second thermal field gives an interface located in a region of concave isotherms. We note however that the interface is concave in each case due to the highly concave nature of the isoconcentration lines. In each thermal field assumed, we find that the interface moves downward from the initial transient region at 32mm along the crystal to a near steady state position at a distance solidified of 101mm. This is consistent with results obtained in a one dimen-

sional diffusion model (6).

4.0 DISCUSSION

We have described a technique by which the solid-liquid interface location and composition may be determined from compositional analysis of a crystal and determination of the thermal profile via suitable thermal models. The resulting interface is consistent with both the experimentally determined solute composition profile and the calculated thermal field. The technique allows for an interface that is neither an isotherm nor an isoconcentrate, and can be used to determine the interface location at any point in the crystal.

In order to be useful in determining the causes of radial segregation in systems such as HgCdTe, we must first ensure that the thermal model adequately describes the thermal conditions encountered during an actual experiment. Thermophysical properties of solid solution semiconductors such as HgCdTe are not well known, and the high vapor pressures encountered prevent a direct measure of the thermal profile with thermocouples. The iteration procedure described in this paper depends on accurate values for both the compositional profile and the thermal profile. The problems encountered in determining the thermal field are the same, however, as encountered in attempting to solve the set of coupled equations described in section 2.

Due to a lack of thermophysical properties for HgCdTe we have not carried out the full iterative procedure necessary to determine an interface consistent with the compositional profile and experimentally measured thermal boundary conditions. By way of example we have illustrated that thermal fields typical of those encountered in real growth situations leads to interface shapes with only a slight degree of curvature being consistent with measured isoconcentration profiles that are highly curved. This indicates that in a system such as HgCdTe, mechanisms that lead to even a slightly curved solid-liquid interface may result in gross radial compositional variations. One such mechanism, that of shape instability, will be addressed in a later paper.

ACKNOWLEDGMENTS

The authors wish to acknowledge numerous constructive discussions with M.C. Davidson, S.L. Lehoczky and F.R. Szofran. This work was funded by NASA contract NAS8-33698. Preliminary experimental work was performed by one of the authors (DCG) while working as a U.S.R.A. Visting Scientist at Marshall Space Flight Center under NASA contract NAS8-33445.

REFERENCES

(1) S. Corriell and R.F. Sekerka, J. Crystal Growth 46 (1979) 479.

(2) S. Corriell, R. F. Boisvert, R. J. Rehm and R.F. Sekerka, J. Crystal Growth 54 (1981 167.

(3) B. E. Bartlett, P. Capper, J.E. Harris and M.J.T. Quelch, J. Crystal Growth 46 (1979) 623.

(4) D. E. Holmes and H.C. Gatos, J. Electrochem. Soc. 128 (1981) 429.

(5) M.C. Davidson, Private Communication

(6) M.H. Burden, D.J. Helditch and J.D. Hunt, J. Crystal Growth 20 (1973) 121.

(7) J. C. Clayton, M.C. Davidson, D.C. Gillies and S.L. Lehoczky, Submitted to J. Crystal Growth.

FIGURE CAPTIONS

FIGURE 1 - Schematic Diagram of Interface Determination Procedure.

FIGURE 2 - Solidus determined from Crystal Composition Data in HgCdTe.

FIGURE 3 - Thermal Profiles Applicable to HgCdTe Growth.

FIGURE 4 - Interface Locations in HgCdTe for Two Assumed Thermal Fields.

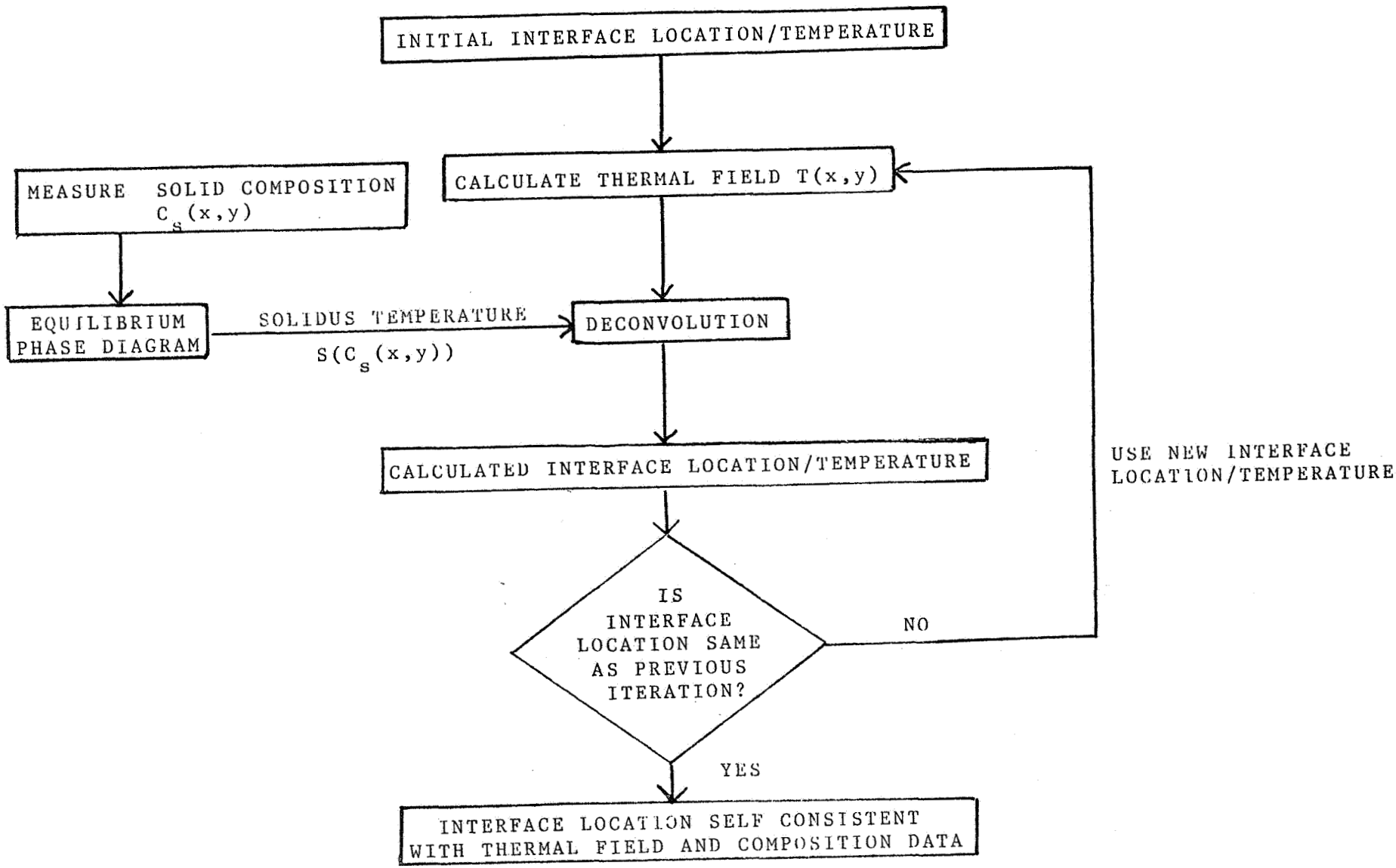

FIGURE 1. SCHEMATIC DIAGRAM OF INTERFACE DETERMINATION PROCEDURE

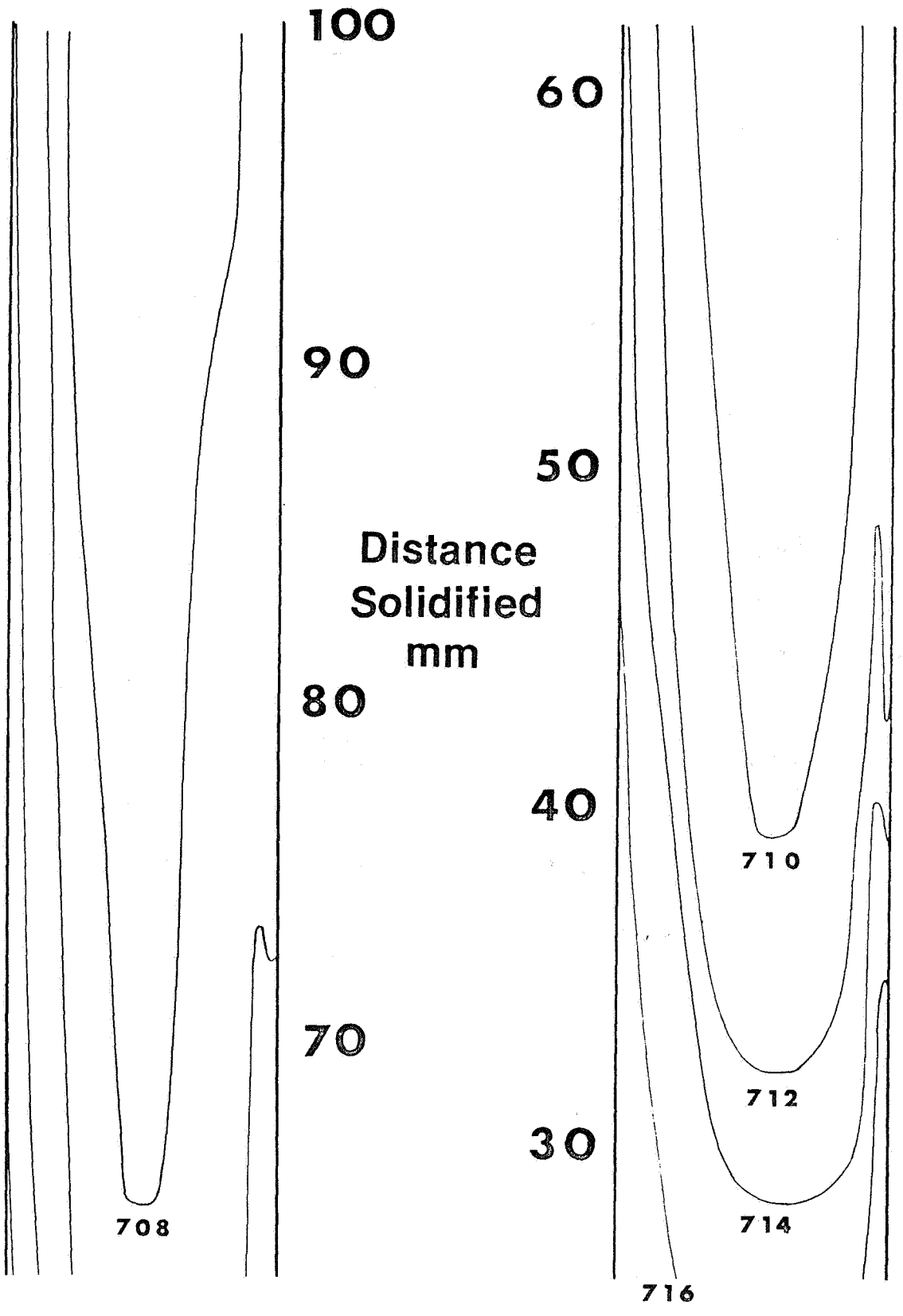
100
90
80
70
60
50
40
30
Distance
Solidified
mm
708
710
712
714
716